

Insight into the prospective evaluation of third-order interelectronic corrections on Li-like ions

R. N. Soguel^{1,2,3,*} and S. Fritzsche^{1,2,3}

¹*Theoretisch-Physikalisches Institut, Friedrich-Schiller-Universität Jena, Max-Wien-Platz 1, 07743 Jena, Germany*

²*Helmholtz-Institut Jena, Fröbelstieg 3, 07743 Jena, Germany*

³*GSI Helmholtzzentrum für Schwerionenforschung GmbH, Planckstraße 1, 64291 Darmstadt, Germany*

(Dated: October 20, 2023)

Relying on the redefined vacuum state approach, and based on one-particle three-loop Feynman diagrams, partial third-order interelectronic corrections to the valence electron energy shift are investigated in Li-like ions. The idea is to begin with simple one-particle gauge-invariant subsets composed of Feynman diagrams and to keep track of them in the many-electron frame, which is a strong asset of the formalism. An independent derivation is undertaken with the help of perturbation theory to cross-check the expressions. This two-method scheme helps to resolve how the different terms are distributed among three- and four-electron contributions. Furthermore, it provides a tool to overcome the difficulties related to the derivation of reducible terms, which are tricky to deal with. These two independent derivations and the comparison of the resulting expressions are fully consistent, except for two expressions. In these cases, the discrepancy can be traced back to a different topology of the poles.

I. INTRODUCTION

Quantum electrodynamics (QED) is the prototype gauge theory on which the Standard Model (SM) of particles relies on. QED has shown to be impressively reliable in its ability to provide accurate predictions. To illustrate, consider the most precise prediction of the SM, the free electron magnetic moment in Bohr magnetons, $g/2$. A recent study measured its value to a spectacular precision of 1.3 parts in 10^{13} [1]. The SM prediction involves three sectors in its evaluation; it receives contributions from QED, as well as from the hadronic and weak interactions. For the former sector, the asymptotic power series in the fine-structure constant α is expanded up to the fifth order [2], and contains muon and tauon contributions. The bound electron magnetic moment is more subtle to assess, nevertheless the stunning accuracy of 5.6 parts in 10^{13} [3] was reached. To arrive at this value, a co-trapping of two different isotopes of neon ions was devised. Moreover, pushing QED in the presence of the binding nuclear field to its limits is a great way to gain in-depth knowledge about the theory and to probe potential new physics [4].

Heavy highly charged ions offer a great natural laboratory to study QED in strong field regimes [5]. Unfortunately, such experimental high precision level is not achieved yet in the transition energies of heavy highly charged ions. Consider as an example the $1s$ Lamb shift in H-like ions, whose experimental value is 460.2 ± 4.6 eV [6]. The comparison between theory and experiment allows to probe first-order QED effects on a 1.7 percent level [5]. In order to test second-order QED effects, which contribute $-1.26(33)$ eV [7], demanding experimental updates are required [8]. A part of the problem lies in the high energy of the transitions involved, where the sensitivity of the detectors is poor in the KeV regime. Note that a lot of energy is required to excite the tightest bound electron over the ionization threshold. A way to circumvent this issue is to probe many-electron transition energies, lying from

soft x-ray to ultraviolet and, accessible by laser spectroscopy. Already for He-like ions, the uncertainties drop below the eV level [9, 10]. In the case of Li-like ions, the accuracy reached the meV level both in uranium [11, 12] and xenon [13] ions. A similar accuracy was achieved in Be-like ions [14]. Also in B-like [15, 16], F-like [17, 18] and Na-like [19] ions precise measurements were conducted. To date, the most compelling experimental cases are found to be (i) the $2p_{3/2} - 2s$ transition in Li-like bismuth ions [20], (ii) the $2p_{1/2} - 2s$ transition in Li-like uranium ions [12].

The increasing experimental precision drives theoretical predictions to their limits and enforces an accurate description of complex electrons dynamics. The evaluation of the dynamical properties and the structure of highly relativistic, tightly bound electrons in highly-charged ions with utmost accuracy represents one of the most important and demanding problems in modern theoretical atomic physics. In this view, the treatment of the interelectronic interaction is a fundament in order to achieve accurate theoretical predictions of the energy levels in many-electron atoms or ions. As a consequence, *ab initio* calculations are the holy grail in the quest for many-electron atoms in the frame of bound-state QED (BSQED). The derivations performed so far used a zeroth-order many-electron wave function constructed as a Slater determinant (or sum of Slater determinants) with all electrons involved [21–23]. Such a derivation becomes increasingly difficult to handle for many-electron systems, especially when facing higher-order corrections. The framework of a vacuum state redefinition [24–26] is proposed to tackle third-order interelectronic interactions. Such a technique is not yet widely spread in the BSQED community but already proved helpful in the evaluation of the screened radiative and two-photon exchange corrections to the g -factor and hyperfine splitting [27–32], the ground-state and ionization energies of Be-like ions [33, 34], respectively, and for the transition energies between low-lying levels [35]. It showed to be of intrinsic relevance in the evaluation of the Delbrück scattering above the pair production threshold [36].

This work treats (a partial) third-order interelectronic correction to a single-valence state over closed-shells. The aim

*Electronic address: romain.soguel@uni-jena.de

is to demonstrate that it is feasible to assess third-order inter-electronic corrections even though such calculations are challenging and especially difficult. To exclude mistakes, and as a cross-check of the derived expressions, two different methods are utilised to obtain the results. The first one is an effective one-particle approach, which relies on the redefinition of the vacuum state. It deals with one-particle three-loop diagrams. Its presentation is given in Sec. III, after a brief introduction to BSQED in Sec. II. The idea is to provide a proof-of-principle that third-order interelectronic corrections can be tackled in the redefined vacuum state framework, owing to the transcription of the one-particle gauge-invariant (GI) subsets to many-electron diagrams. The second method, introduced in Sec. IV, considers a perturbation theory approach to a two-photon-exchange subset. The subset involves a loop contribution, and a potential-like interaction accounts for the perturbation. Then, the results are mapped to the three-photon-exchange corrections. This independent derivation of the formulas ensures that potential mistakes are identified and ruled out. The resulting expressions contain infrared (IR) divergences. These are inspected in Sec. V, regularized by the introduction of a photon mass term, and it is shown that they are cancelled by terms within the proposed GI subsets. Section VI compares the outcomes of the two methods. The present work ends with a concluding discussion in Sec. VII.

Natural units ($\hbar = c = m_e = 1$) are used throughout this paper, the fine structure constant is defined as $\alpha = e^2/(4\pi)$, $e < 0$. Unless explicitly stated, all integrals are implicitly assumed to be over the full real axis.

II. BOUND STATE QED

The relativistic quantum description of the electron-positron field is based on the Dirac equation. The framework of BSQED is based on the resummation of all Feynman diagrams involving the interaction of the (free) electron with the classical field of the nucleus. Such a procedure, applied by Weinberg [37], leads to the bound-state electron propagator. Equivalently, from Furry's perspective [38], the interaction of the electron-positron field with the external classical field of the nucleus can also be taken into account non-perturbatively from the beginning by solving Dirac equation in the presence of the binding potential,

$$h_D \phi_j(\mathbf{x}) = [-i\boldsymbol{\alpha} \cdot \boldsymbol{\nabla} + \beta + V(\mathbf{x})] \phi_j(\mathbf{x}) = \epsilon_j \phi_j(\mathbf{x}), \quad (1)$$

leading to the so-called Furry picture of QED. $\phi_j(\mathbf{x})$ are the solutions of the stationary Dirac equation in the potential well $V(\mathbf{x})$ occurring due to the nucleus and j stands for all quantum numbers. α^k and β are Dirac matrices, $V(\mathbf{x}) = V_C(\mathbf{x})$ is the external classical Coulomb field arising from the nucleus. Solving Eq. 1 implies an all-order treatment in αZ , with Z the nuclear charge, hence going beyond perturbative regime. The time-depend solution is the stationary solution $\phi_k(\mathbf{x})$ multiplied by the phase factor $\exp(-i\epsilon_k t)$. For completeness, the extended Furry picture accounts for the presence of a screening potential $U(\mathbf{x})$ besides the Coulomb one, $V(\mathbf{x}) = V_C(\mathbf{x}) + U(\mathbf{x})$, which implies a partial consideration

of interelectronic interactions. The redefinition of the vacuum state is conducted in such a way that all core orbitals from the closed shells belong to it [39]. The notation $|\alpha\rangle$ stands for

$$|\alpha\rangle = a_a^\dagger a_b^\dagger a_c^\dagger \dots |0\rangle, \quad (2)$$

and $|\alpha\rangle$ is going to be referred to as the redefined vacuum state. The following notation is applied, according to Lindgren and Morisson [39] and Johnson [40]: v designates a valence electron, a, b, c, \dots stands for core orbitals, i, j, k, l, p, \dots correspond to arbitrary states. Upon second quantization, the (non-interacting) electron-positron field can be expanded in terms of creation and annihilation operators. Within the redefined vacuum state approach, such decomposition still holds but needs to be slightly adapted with respect to the Fermi level E_α^F ,

$$\psi_\alpha^{(0)}(t, \mathbf{x}) = \sum_{\epsilon_j > E_\alpha^F} a_j \phi_j(\mathbf{x}) e^{-i\epsilon_j t} + \sum_{\epsilon_j < E_\alpha^F} b_j^\dagger \phi_j(\mathbf{x}) e^{-i\epsilon_j t}. \quad (3)$$

The Fermi level of the redefined vacuum state lies between the highest core state and the valence state, $E_\alpha^F \in (\epsilon_a, \epsilon_v)$. Consequently, the electron propagator is affected in the following manner,

$$\begin{aligned} \langle \alpha | T \left[\psi_\alpha^{(0)}(t, \mathbf{x}) \bar{\psi}_\alpha^{(0)}(t', \mathbf{y}) \right] | \alpha \rangle = \\ = \frac{i}{2\pi} \int d\omega \sum_j \frac{\phi_j(\mathbf{x}) \bar{\phi}_j(\mathbf{y}) e^{-i(t-t')\omega}}{\omega - \epsilon_j + i\varepsilon(\epsilon_j - E_\alpha^F)}, \end{aligned} \quad (4)$$

where $\epsilon > 0$ implies the limit to zero. It is convenient to define $u = 1 - i\varepsilon$ for later use. The difference between the electron propagator in the redefined vacuum and in the standard one corresponds graphically to a cut of an inner electron line in the Feynman diagram. Such difference is mathematically implemented via the Sokhotski-Plemelj theorem. For $p \in \mathbb{N}^*$,

$$\begin{aligned} \sum_j \frac{\phi_j(\mathbf{x}) \bar{\phi}_j(\mathbf{y})}{[\omega - \epsilon_j + i\varepsilon(\epsilon_j - E_\alpha^F)]^p} \\ - \sum_j \frac{\phi_j(\mathbf{x}) \bar{\phi}_j(\mathbf{y})}{[\omega - \epsilon_j + i\varepsilon(\epsilon_j - E^F)]^p} \\ = \frac{2\pi i (-1)^p}{(p-1)!} \frac{d^{(p-1)}}{d\omega^{(p-1)}} \sum_a \delta(\omega - \epsilon_a) \phi_a(\mathbf{x}) \bar{\phi}_a(\mathbf{y}), \end{aligned} \quad (5)$$

this equality is to be understood while integrating in the complex ω -plane. The reader is referred to Refs. [25, 26, 41] for more details on the vacuum state redefinition within the BSQED framework and the corresponding formalism.

The light-unperturbed normal ordered Hamiltonian can be expressed as [42]

$$H_0 = \int d^3\mathbf{x} : \psi^{(0)\dagger}(t, \mathbf{x}) h_D \psi^{(0)}(t, \mathbf{x}) : . \quad (6)$$

It is left to introduce the light related part. The interaction Hamiltonian is constructed as

$$H_{\text{int}} = \int d^3\mathbf{x} : \psi^{(0)\dagger}(t, \mathbf{x}) h_{\text{int}} \psi^{(0)}(t, \mathbf{x}) : . \quad (7)$$

It encapsulates the interaction with the quantized electromagnetic field A_μ and the counterterm associated to the screening potential $-U(\mathbf{x})$, when one works within the extended Furry picture. The explicitly expression for h_{int} is $h_{\text{int}} = e\alpha^\mu A_\mu(t, \mathbf{x}) - U(\mathbf{x})$. The effect of the interaction Hamiltonian is accounted for within BSQED perturbation theory. Different approaches are possible for its formulation [24, 42–44]. The calculation presented in what follows relies on the two-time Green’s function (TTGF) method [24].

The photon propagator is denoted by $D_{\mu\nu}(\mathbf{x}-\mathbf{y}; \omega)$, with ω the photon’s energy. The interelectronic-interaction operator $I(\mathbf{x}-\mathbf{y}; \omega)$ is defined as $I(\mathbf{x}-\mathbf{y}; \omega) = e^2\alpha^\mu\alpha^\nu D_{\mu\nu}(\mathbf{x}-\mathbf{y}; \omega)$, where $\alpha^\mu = (1, \boldsymbol{\alpha})$. The interelectronic-interaction matrix element $I_{ijkl}(\omega)$ is a shorthand notation standing for

$$I_{ijkl}(\omega) = \int d^3\mathbf{x}d^3\mathbf{y}\psi_i^\dagger(\mathbf{x})\psi_j^\dagger(\mathbf{y})I(\mathbf{x}-\mathbf{y}; \omega)\psi_k(\mathbf{x})\psi_l(\mathbf{y}), \quad (8)$$

and satisfies the transposition symmetry property $I_{ijkl}(\omega) = I_{jilk}(\omega)$. In the Feynman and Coulomb gauges, the interelectronic-interaction operator $I(\mathbf{x}-\mathbf{y}; \omega)$ is an even function of ω .

III. REDEFINED VACUUM STATE APPROACH

The idea behind a redefinition of the vacuum state is to benefit from a hydrogen-like picture of the problem, the system for which QED is the most developed. This setting is feasible as long as the system under consideration has a single valence electron above some closed shells. The essential notion in introducing a redefined vacuum state is to separate the electron dynamics into the “core” and “valence” parts. The first part is relegated to the reference vacuum energy and can be neglected when the transition energy – with a significant many-electron background remaining unchanged – is considered. The key feature of this approach is that the core contributions – arising from the interaction between core electrons are canceled in the difference between the excited and the ground state energies – are not considered from the very beginning.

The effective one-particle approach, based on a redefinition of the vacuum state, is applied here to more involved Feynman diagrams, as a proof-of-principle that advanced calculation

can be undertaken in this way. The three-photon-exchange corrections investigated, as well as the specific one-particle three-loop Feynman diagrams serving as a starting point of the subsequent consideration were selected with hindsight. It was necessary to be able to verify, in some manner, the obtained expressions. The perturbative approach requires already known diagrams, therefore, some totally new topology in the considered diagrams was not a realistic choice such as for example, a one-loop correction shared among three electrons exists. Hence, after the introduction of the necessary elements of the TTGF method, a partial recap on the two-photon-exchange correction is undertaken. It both details how the investigated diagrams were selected and serves as a starting point for later developments.

The investigation is carried out for the valence state described as $|v\rangle = a_v^\dagger|\alpha\rangle$ in the perspective of a redefined vacuum state. The cornerstone expression for the energy shift is

$$\Delta E_v = \frac{\frac{1}{2\pi i} \oint_{\Gamma_v} dE(E - \langle v|H_0|v\rangle) \langle v|\Delta g_\alpha(E)|v\rangle}{1 + \frac{1}{2\pi i} \oint_{\Gamma_v} dE \langle v|\Delta g_\alpha(E)|v\rangle}, \quad (9)$$

where the contour Γ_v is chosen such that it surrounds anticlockwise only the pole $E^{(0)} = \langle v|H_0|v\rangle \equiv \epsilon_v$. Other singularities are kept outside this contour. The Fourier transformed TTGF matrix element is provided by $\langle v|\Delta g_\alpha(E)|v\rangle = \Delta g_{\alpha, vv}$, where $\Delta g_\alpha(E)$ stands for $\Delta g_\alpha(E) = g_\alpha(E) - g_\alpha^{(0)}(E)$ and $g_\alpha^{(0)}(E)$ is the zeroth-order Fourier transformed TTGF. The Fourier transformed TTGF, where the coordinates have been integrated out, is given by

$$g_\alpha(E)\delta(E - E') = \frac{1}{2\pi i} \sum_{i,j} \int d^3x d^3y \int dt dt' e^{i(Et - E't')} \times \phi_i^\dagger(\mathbf{x}) \langle \alpha|T[\psi_\alpha(t, \mathbf{x})\psi_\alpha^\dagger(t', \mathbf{y})]|\alpha\rangle \phi_j(\mathbf{y}) a_i^\dagger a_j. \quad (10)$$

The treatment of the Green’s function within perturbation theory allows to expand it to the different orders in α : $\Delta g_\alpha(E) = \Delta g_\alpha^{(1)}(E) + \Delta g_\alpha^{(2)}(E) + \Delta g_\alpha^{(3)}(E) + \dots$. Isolating the corresponding third order, the resulting expression for the energy shift can be represented as

$$\Delta E_v^{(3)} = \frac{1}{2\pi i} \oint_{\Gamma_v} dE(E - \epsilon_v)\Delta g_{\alpha, vv}^{(3)}(E) - \frac{1}{2\pi i} \oint_{\Gamma_v} dE(E - \epsilon_v)\Delta g_{\alpha, vv}^{(2)}(E) \frac{1}{2\pi i} \oint_{\Gamma_v} dE' \Delta g_{\alpha, vv}^{(1)}(E') - \frac{1}{2\pi i} \oint_{\Gamma_v} dE(E - \epsilon_v)\Delta g_{\alpha, vv}^{(1)}(E) \left\{ \frac{1}{2\pi i} \oint_{\Gamma_v} dE' \Delta g_{\alpha, vv}^{(2)}(E') - \left[\frac{1}{2\pi i} \oint_{\Gamma_v} dE' \Delta g_{\alpha, vv}^{(1)}(E') \right]^2 \right\}. \quad (11)$$

The terms which do not involve $\Delta g_{\alpha, vv}^{(3)}(E)$ are referred to as disconnected elements. A peculiar attention is required in the treatment of the contributions where the energy of an interme-

diated state equals to the energy of the reference state. These type of contributions are so-called *reducible* terms. Three different type of Feynman diagrams are found at this order and

are separated accordingly as follows: the one-particle loop diagrams are denoted by (L), the interelectronic-interaction diagrams by (I) and the screened-loop diagrams by (S). This reports focuses on the third-order interelectronic interactions (I), also referred to as three-photon-exchange corrections.

A. Partial recap on two-photon-exchange corrections

To showcase that the vacuum state redefinition approach is working, one resorts to results from Ref. [25]. The two-photon-exchange corrections were derived within the framework of a vacuum state redefinition, thus starting from an effective one-particle picture.

The complete set of second-order one-particle diagrams consists of ten two-loop diagrams. These are presented in Fig. 1. The gauge invariance of the one-particle two-loop diagrams was shown in Ref. [45]. Eight gauge invariant subsets are identified based on the decomposition provided in this paper. The identified subsets should be gauge invariant in both the redefined and the standard vacuum state frameworks. This means that the many-electron diagrams obtained as a difference between redefined and standard vacuum state diagrams can be also classified according to these subsets. The subsets are labelled according to their composition in radiative-loop corrections. In what follows, SE stands for the *self-energy* loop and VP for the *vacuum-polarization* loop. The subsets, with the labeling presented in Figs. 1, are the SESE one in the first line, the SEVP one in the second line, and the VPVP, V(VP)P, V(SE)P, and S(VP)E ones, from left to right, in the third line. The eight identified GI subsets in the original Furry picture are, in terms of the one-electron description: SESE (two- and three-electron subsets), SEVP, S(VP)E (two- and three-electron subsets), VPVP, V(VP)P, and V(SE)P.

The resulting two-photon-exchange corrections are divided into three categories, in the many-electron frame; the ladder diagram (referred to as ladder loop), the crossed-ladder diagram (referred to as the crossed loop) and the three-electron diagram (referred to as the three-electron term in this subsection).

It was shown that that the ladder- and crossed-loop arose from the SESE and S(VP)E subsets [46]. The SESE subset generates the exchange parts of the two-photon-exchange corrections, whereas the S(VP)E subset generates the direct parts of the two-photon-exchange corrections. The decision was made to pick out the S(VP)E subset as a starting point of the third-order interelectronic corrections. The reasons are (i) its simplicity in terms of the number of diagrams to consider (3 vs 1), and (ii) the fact that dealing with the exchange part is more difficult. The one-particle three-loop Feynman diagrams are given in Figs. 2 [S[V(VP)P]E subset] and 3 [S(VP)EVP subset]. They correspond to all possible insertion of a VP loop in the S(VP)E graph, being the simplest extension towards a one-loop three-photon-exchange corrections. Note that the inclusion of an extra energy-independent interelectronic operator, arising from the cut in the inserted VP loop, does not spoil gauge invariance. The one-photon-exchange operator was shown to be gauge invariant [25]. An important point

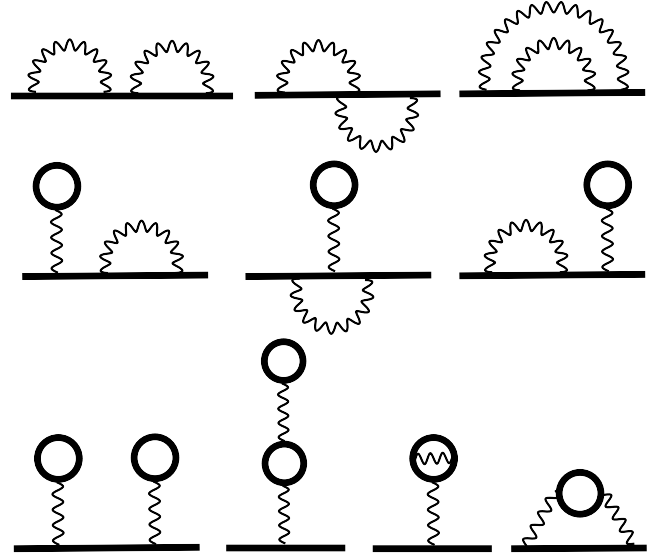


FIG. 1: The second-order one-electron Feynman diagrams labeled as follows: SESE (first row); SEVP (second row); VPVP, V(VP)P, V(SE)P, and S(VP)E from left to right in the last row. Thick black lines denote the electron propagator in the redefined vacuum state in an external potential V . Wavy lines represent to the photon propagator.

to highlight is that the ω -flow in the VP loop must be symmetrized in the integrals of the final expressions in order to achieve gauge invariance. It was a crucial step when dealing with the S(VP)E subset (as shown below). The equality (16), and its third-order-pole version, were applied to the derived expressions in order to compare them with those based on the perturbation theory approach.

The expressions related to the S(VP)E subset are displayed below, as the initial expressions for later derivations based on perturbation theory. The proof for the gauge invariance of the S(VP)E subset is given numerically, for the Feynman and Coulomb gauges, in Tables I and II at the corresponding lines, and analytically in Eq. (67) for the three-electron terms in Ref. [25]. The two-electron irreducible part $\Delta E_v^{(21)S(VP)E,2e,irr}$ reads

$$\Delta E_v^{(21)S(VP)E,2e,irr} = \frac{i}{2\pi} \int d\omega \left[\sum'_{a,i,j} \frac{I_{vja}(\omega) I_{iav}(\omega)}{(\epsilon_v - \omega - \epsilon_i u)(\epsilon_a - \omega - \epsilon_j u)} + \sum_{a,i,j}^{(i,j) \neq (a,v)} \frac{I_{vai}(\omega) I_{ijva}(\omega)}{(\epsilon_v - \omega - \epsilon_i u)(\epsilon_a + \omega - \epsilon_j u)} \right], \quad (12)$$

where one excludes the contribution with $\epsilon_i = \epsilon_v$ and $\epsilon_j = \epsilon_a$ from the crossed-direct term (first item) by hand and note this by the prime on the sum. The two-electron reducible part $\Delta E_v^{(21)S(VP)E,2e,red}$, coming from the ladder direct restriction $\epsilon_i + \epsilon_j = \epsilon_a + \epsilon_v$ together with the excluded part from the

irreducible crossed-direct term, yields

$$\begin{aligned} \Delta E_v^{(2)S(VP)E,2e,\text{red}} = & \\ & - \frac{i}{4\pi} \int d\omega \left[\frac{1}{(\omega + i\varepsilon)^2} + \frac{1}{(-\omega + i\varepsilon)^2} \right] \\ & \times \sum_{a,a_1,v_1} I_{vaa_1v_1}(\Delta_{va} - \omega) I_{a_1v_1va}(\Delta_{va} - \omega). \end{aligned} \quad (13)$$

The three-electron irreducible part $\Delta E_v^{(2)S(VP)E,3e,\text{irr}}$ yields

$$\begin{aligned} \Delta E_v^{(2)S(VP)E,3e,\text{irr}} = & \\ & - \sum_{a,b,i}^{(i,b) \neq (v,a)} \frac{I_{vabi}(\Delta_{vb}) I_{biva}(\Delta_{vb}) + I_{vai b}(\Delta_{ba}) I_{ibva}(\Delta_{ba})}{(\epsilon_v + \epsilon_a - \epsilon_b - \epsilon_i)} \\ & - \sum_{a,b,i} \frac{I_{viba}(\Delta_{vb}) I_{bavi}(\Delta_{vb})}{(\epsilon_a + \epsilon_b - \epsilon_v - \epsilon_i)}, \end{aligned} \quad (14)$$

together with the corresponding reducible part,

$$\Delta E_v^{(2)S(VP)E,3e,\text{red}} = - \sum_{a,a_1,v_1} I_{vaa_1v_1}(\Delta_{va}) I'_{a_1v_1va}(\Delta_{va}). \quad (15)$$

As a side remark, note that the identity

$$\frac{-1}{(x + i\varepsilon)^2} + \frac{1}{(-x + i\varepsilon)^2} = \frac{2\pi}{i} \partial_x \delta(x) \quad (16)$$

was used to symmetrize the ω -flow in the VP loop, or in other words, to symmetrize the pole structure with respect to the real-line axis.

B. S[V(VP)P]E subset

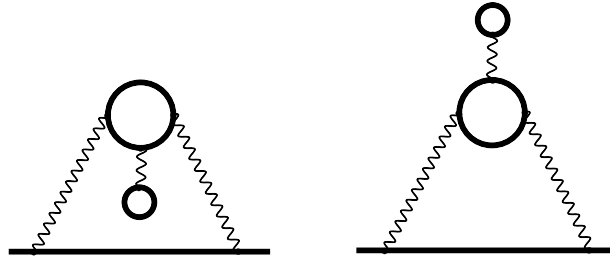


FIG. 2: One-particle three-loop Feynman diagrams of the S[V(VP)P]E subset participating to the third-order contribution to the energy shift of a single-particle state. They are denoted by H_1 (left) and H_2 (right). Notations are the same as in Fig. 1.

The Green's function corresponding to each diagram in the subset are given by

$$\begin{aligned} \Delta g_{\alpha, vv}^{(3)H_1}(E) = & \frac{1}{(E - \epsilon_v)^2} \left(\frac{i}{2\pi} \right)^3 \sum_{i,j,k,l,p} \int d\omega dk_1 dk_2 \frac{I_{vpik}(\omega)}{[E - \omega - \epsilon_i + i\varepsilon(\epsilon_i - E_\alpha^F)][k_1 - \epsilon_j + i\varepsilon(\epsilon_j - E_\alpha^F)]} \\ & \times \frac{I_{kjlj}(0) I_{lipv}(\omega)}{[k_2 - \epsilon_k + i\varepsilon(\epsilon_k - E_\alpha^F)][k_2 - \epsilon_l + i\varepsilon(\epsilon_l - E_\alpha^F)][k_2 - \omega - \epsilon_p + i\varepsilon(\epsilon_p - E_\alpha^F)]}, \end{aligned} \quad (17)$$

for H_1 and by

$$\begin{aligned} \Delta g_{\alpha, vv}^{(3)H_2}(E) = & \frac{1}{(E - \epsilon_v)^2} \left(\frac{i}{2\pi} \right)^3 \sum_{i,j,k,l,p} \int d\omega dk_1 dk_2 \frac{I_{vki j}(\omega)}{[E - \omega - \epsilon_i + i\varepsilon(\epsilon_i - E_\alpha^F)][k_1 - \epsilon_j + i\varepsilon(\epsilon_j - E_\alpha^F)]} \\ & \times \frac{I_{lpkp}(0) I_{jilv}(\omega)}{[k_1 - \omega - \epsilon_k + i\varepsilon(\epsilon_k - E_\alpha^F)][k_1 - \omega - \epsilon_l + i\varepsilon(\epsilon_l - E_\alpha^F)][k_2 - \epsilon_p + i\varepsilon(\epsilon_p - E_\alpha^F)]}. \end{aligned} \quad (18)$$

for H_2 . According to the line of reasoning presented in the treatment of the SESE subset in Ref. [25], starting from the previous Green's functions, the extraction of the different three-photon-exchange corrections is carried out with the

subtraction of the corresponding expression in the standard vacuum state

$$\Delta E_v^{(3)} - \Delta E_v^{(3L)} = \Delta E_v^{(3I)} + \Delta E_v^{(3S)}. \quad (19)$$

In other words, within the framework of a redefined vacuum state, the interelectronic and the screened corrections are treated on the same footing. As the diagrams are one-particle irreducible (1PI), one does not need to worry about the disconnected elements in Eq. (11). Note that double cuts are possible in both diagrams, leading to so called non-diagrammatic elements. These are important to consider in order to properly treat the reducible part. Non-diagrammatic elements are expressions that cannot be drawn as single Feynman diagrams since they involve reducible parts. The results are separated in three- and four-electron contributions.

To illustrate the extraction procedure based on Eq. (19),

the term-by-term three-electron (loop diagram) expressions obtained afterwards are displayed explicitly below for H_1 . One distinguishes between three different type of terms: irreducible (irr), reducible 1 (red1) and reducible 2 (red2). The irreducible terms correspond to a first order pole (S -matrix terms) in the first expression of Eq. (11), whereas the reducible 1 and 2 terms correspond to a second and third order pole, respectively, in the first expression of Eq. (11). To keep track of the source of generated reducible parts, a subscript is used with previous notation; for example, v_1, a_1, b_2 , where $\epsilon_{i_1} = \epsilon_i$. The different terms corresponding to crossed graphs are found to be

$$\Delta E_{v, H_1}^{(3I)3e, \text{cross}, \text{irr}} = \frac{i}{2\pi} \int d\omega \sum_{i,j,k}^{k \neq b} \frac{I_{vjib}(\omega) I_{baka}(0) I_{kijv}(\omega)}{(\epsilon_v - \omega - \epsilon_i u)(\epsilon_b - \omega - \epsilon_j u)(\epsilon_b - \epsilon_k u)}, \quad (20)$$

$$\Delta E_{v, H_1}^{(3I)3e, \text{cross}, \text{irr}} = \frac{i}{2\pi} \int d\omega \sum_{i,j,k}^{k \neq b} \frac{I_{vjik}(\omega) I_{kaba}(0) I_{bijv}(\omega)}{(\epsilon_v - \omega - \epsilon_i u)(\epsilon_b - \omega - \epsilon_j u)(\epsilon_b - \epsilon_k u)}. \quad (21)$$

The terms associated to ladder graphs are given as follows,

$$\Delta E_{v, H_1}^{(3I)3e, \text{lad}, \text{irr}} = \frac{i}{2\pi} \int d\omega \sum_{i,j,k}^{\{i,j\} \neq \{v,b\}, \{i,k\} \neq \{v,b\}} \frac{I_{vbij}(\omega) I_{jaka}(0) I_{kibv}(\omega)}{(\epsilon_v - \omega - \epsilon_i u)(\epsilon_b + \omega - \epsilon_j u)(\epsilon_b + \omega - \epsilon_k u)}, \quad (22)$$

$$\Delta E_{v, H_1}^{(3I)3e, \text{lad}, \text{red1}} = -\frac{i}{2\pi} \int d\omega \sum_{i,j,k}^{\{i,j\} = \{v,b\}, \{i,k\} \neq \{v,b\}} \frac{I_{vbij}(\omega) I_{jaka}(0) I_{kibv}(\omega)}{(\epsilon_v - \omega - \epsilon_i u)^2 (\epsilon_b + \omega - \epsilon_k u)}, \quad (23)$$

$$\Delta E_{v, H_1}^{(3I)3e, \text{lad}, \text{red1}} = -\frac{i}{2\pi} \int d\omega \sum_{i,j,k}^{\{i,j\} \neq \{v,b\}, \{i,k\} = \{v,b\}} \frac{I_{vbij}(\omega) I_{jaka}(0) I_{kibv}(\omega)}{(\epsilon_v - \omega - \epsilon_i u)^2 (\epsilon_b + \omega - \epsilon_j u)}, \quad (24)$$

$$\Delta E_{v, H_1}^{(3I)3e, \text{lad}, \text{red2}} = \frac{i}{2\pi} \int d\omega \sum_{i,j,k}^{\{i,j\} = \{v,b\}, \{i,k\} = \{v,b\}} \frac{I_{vbij}(\omega) I_{jaka}(0) I_{kibv}(\omega)}{(\epsilon_v - \omega - \epsilon_i u)^3}. \quad (25)$$

The non-diagrammatic element for H_1 reads

$$\Delta E_{v, H_1}^{(3I)3e, \text{cross}, \text{red1}} = -\frac{i}{2\pi} \int d\omega \sum_{i,j} \frac{I_{vjib}(\omega) I_{bab_1 a}(0) I_{b_1 i j v}(\omega)}{(\epsilon_v - \omega - \epsilon_i u)(\epsilon_b - \omega - \epsilon_j u)^2}. \quad (26)$$

The expressions presented above are the bare results after carrying out the difference of the vacuum states to extract the interelectronic interactions. We emphasize that the reducible expressions are IR divergent. These IR divergences are extracted and regularized later on, such as the symmetrization of the poles with regard to the real axis. The term-by-term interelectronic expressions related to H_2 are given in Appendix A. They are needed to show the explicit cancellation of IR divergences at the single Feynman diagram level. The final interelectronic three-electron expressions are found in Appendix C, when the comparison with the results obtained from the perturbation theory approach is made. The four-electron terms are displayed in Appendix D, again for a comparison with the outcome of the second method.

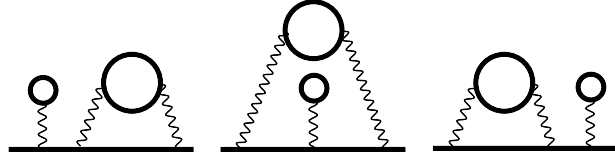


FIG. 3: One-particle three-loop Feynman diagrams of the S(VP)EVP subset participating to the third-order contribution to the energy shift of a single-particle state. They are denoted by F_1 (left), F_2 (middle) and F_3 (right). Notations are similar to Fig. 1.

C. S(VP)EVP subset

As a second example, consider the Green's function associated to F_2 diagram

$$\Delta g_{\alpha, vv}^{(3)F_2}(E) = \frac{1}{(E - \epsilon_v)^2} \left(\frac{i}{2\pi} \right)^3 \sum_{i,j,k,l,p} \int d\omega dk_1 dk_2 \frac{I_{vtil}(\omega)}{[E - \omega - \epsilon_i + i\varepsilon(\epsilon_p - E_\alpha^F)][k_1 - \epsilon_j + i\varepsilon(\epsilon_j - E_\alpha^F)]} \\ \times \frac{I_{ijkj}(0)I_{kpv}(\omega)}{[E - \omega - \epsilon_k + i\varepsilon(\epsilon_p - E_\alpha^F)][k_2 - \epsilon_l + i\varepsilon(\epsilon_l - E_\alpha^F)][k_2 - \omega - \epsilon_p + i\varepsilon(\epsilon_p - E_\alpha^F)]}. \quad (27)$$

The identical procedure as stated above is applied to infer the three-photon-exchange corrections. The diagrams are not 1PI, with the exception of F_2 . Therefore, one has to consider the second-order Green's function $\Delta g_\alpha^{(2)S(VP)E}$ and the first-order one $\Delta g_\alpha^{(1)VP}$ to evaluate the disconnected elements in Eq. (11). It turns out that only the first part of the fourth line survives. The disconnected elements are important to account for as they remove the redundancies in the reducible parts. To illustrate, F_1 and F_3 give redundant reducible terms, but the disconnected elements remove the extra ones, coming from F_1 in this case. A small subtlety is nevertheless present if an extra pole is explicitly extracted. In such a case, this re-

ducible term is kept for two reasons. First it cannot be generated in the disconnected ones, and second, which is more important, to achieve the IR finiteness of the expressions in the subset. Hence, for the S(VP)EVP subset, on the top of the peculiar extra-pole-term arising from F_1 , only the F_2 and F_3 reducible IR divergent expressions are displayed in Table I. Non-diagrammatic elements are only present in the F_2 diagram, and are of four-electron type. The results are separated in three- and four-electron contributions. The Feynman diagram F_2 leads to the subsequent expressions. Only an expression associated to a crossed-loop graph is found

$$\Delta E_{v, F_2}^{(3I)3e, cross} = \frac{i}{2\pi} \int d\omega \sum_{i,j,k} \frac{I_{v kib}(\omega)I_{iaja}(0)I_{bjkv}(\omega)}{(\epsilon_v - \omega - \epsilon_i u)(\epsilon_v - \omega - \epsilon_j u)(\epsilon_b - \omega - \epsilon_k u)}, \quad (28)$$

so it is for the ladder-loop graph, but incorporating the different types of terms (irr, red1 and red2) stated above

$$\Delta E_{v, F_2}^{(3I)3e, lad, irr} = \frac{i}{2\pi} \int d\omega \sum_{i,j,k}^{\{i,k\} \neq \{v,b\}, \{j,k\} \neq \{v,b\}} \frac{I_{vbik}(\omega)I_{iaja}(0)I_{kjbv}(\omega)}{(\epsilon_v - \omega - \epsilon_i u)(\epsilon_v - \omega - \epsilon_j u)(\epsilon_b + \omega - \epsilon_k u)}, \quad (29)$$

$$\Delta E_{v, F_2}^{(3I)3e, lad, red1} = -\frac{i}{2\pi} \int d\omega \sum_{i,j,k}^{\{i,k\} = \{v,b\}, \{j,k\} \neq \{v,b\}} \left\{ \frac{I_{vbik}(\omega)I_{iaja}(0)I_{kjbv}(\omega)}{(\epsilon_v - \omega - \epsilon_j u)^2} \left[\frac{1}{(\epsilon_v - \omega - \epsilon_i u)} + \frac{1}{(\epsilon_b + \omega - \epsilon_k u)} \right] \right. \\ \left. + \frac{I_{vbik}(\omega)I_{iaja}(0)I_{kjbv}(\omega)}{(\epsilon_v - \omega - \epsilon_i u)^2(\epsilon_v - \omega - \epsilon_j u)} \right\}, \quad (30)$$

$$\Delta E_{v, F_2}^{(3I)3e, lad, red1} = -\frac{i}{2\pi} \int d\omega \sum_{i,j,k}^{\{i,k\} \neq \{v,b\}, \{j,k\} = \{v,b\}} \left\{ \frac{I_{vbik}(\omega)I_{iaja}(0)I_{kjbv}(\omega)}{(\epsilon_v - \omega - \epsilon_i u)^2} \left[\frac{1}{(\epsilon_v - \omega - \epsilon_j u)} + \frac{1}{(\epsilon_b + \omega - \epsilon_k u)} \right] \right. \\ \left. + \frac{I_{vbik}(\omega)I_{iaja}(0)I_{kjbv}(\omega)}{(\epsilon_v - \omega - \epsilon_i u)(\epsilon_v - \omega - \epsilon_j u)^2} \right\}, \quad (31)$$

$$\Delta E_{v, F_2}^{(31)3e, \text{lad}, \text{red}2} = \frac{i}{2\pi} \int d\omega \sum_{i,j,k}^{\{i,k\}=\{v,b\}, \{j,k\}=\{v,b\}} \left\{ -\frac{I_{vbik}(\omega)I_{iaja}(0)I_{kjbv}(\omega)}{(\epsilon_v - \omega - \epsilon_i u)(\epsilon_v - \omega - \epsilon_j u)} \left[\frac{1}{(\epsilon_v - \omega - \epsilon_i u)} + \frac{1}{(\epsilon_v - \omega - \epsilon_j u)} \right] + \frac{I_{vbik}(\omega)I_{iaja}(0)I_{kjbv}(\omega)}{(\epsilon_v - \omega - \epsilon_i u)^3} \right\}. \quad (32)$$

As in the case of the S[V(VP)P]E subset, the expressions showed above are those obtained in the extraction procedure of the interelectronic interaction, as the difference of the vacuum states. Some more work is required to extract the IR divergences of the reducible terms, to regularize them, as well as to symmetrize the poles with regard to the real axis. The expressions associated to F_1 and F_3 diagrams are found in Appendix B. The explicit cancellation of IR divergences at the single diagram level requires them. The final expressions associated to the one-loop three-photon-exchange diagrams are found in Appendix C, when comparing with the results from the second derivation. The four-electron terms are displayed, for a comparison with the perturbation theory approach, in Appendix D.

IV. PERTURBATION THEORY APPROACH

The idea behind this approach is to perturb a two-photon-exchange correction by the presence of some potential-like

interaction \mathcal{V} , to its first order. This method was applied in Ref. [47] to generate the two-photon-exchange corrections to the g -factor of Li-like ions. Specifically, the one-electron external wave function is perturbed as

$$|i\rangle \rightarrow |i\rangle + |\delta i\rangle, \quad |\delta i\rangle = \sum_{j \neq i} \frac{|j\rangle \mathcal{V}_{ji}}{\epsilon_i - \epsilon_j}, \quad (33)$$

the energy accordingly to

$$\epsilon_i \rightarrow \epsilon_i + \delta\epsilon_i, \quad \delta\epsilon_i = \mathcal{V}_{ii}, \quad (34)$$

leading to the perturbation in the argument of the interelectronic operator

$$I(\Delta_{va}) \rightarrow I(\Delta_{va} + \delta\Delta_{va}) \approx I(\Delta_{va}) + I'(\Delta_{va})(\delta\epsilon_v - \delta\epsilon_a). \quad (35)$$

The notation Δ_{va} stands for $\Delta_{va} = \epsilon_v - \epsilon_a$. The electron propagator (4) involved in the loops has to be perturbed as well. In its energy-position representation, one finds

$$S_{\delta\mathcal{V}}(\epsilon_k \pm \omega; \mathbf{x}, \mathbf{y}) = \delta_{\mathcal{V}} \left(\sum_i \frac{|i\rangle \langle i|}{\epsilon_k \pm \omega - \epsilon_i u} \right) = \sum_{i,j} \frac{|i\rangle \mathcal{V}_{ij} \langle j|}{(\epsilon_k \pm \omega - \epsilon_i u)(\epsilon_k \pm \omega - \epsilon_j u)} - \sum_i \frac{|i\rangle \mathcal{V}_{kk} \langle i|}{(\epsilon_k \pm \omega - \epsilon_i u)^2}. \quad (36)$$

It is a slight generalization of the propagator found in Ref. [48]. This expression is also valid when $\omega = 0$, namely for the four-electron case. However, one should distinguish when to use each of the two terms. If both parentheses $(\epsilon_k \pm \omega - \epsilon_{i,j} u)|_{\omega=0}$ are non-zero, then the first piece of the perturbed propagator is to be used. If one of the parenthesis $(\epsilon_k \pm \omega - \epsilon_{i,j} u)|_{\omega=0}$ is zero, then the second piece of the perturbed propagator is to be used, with the appropriate index. In such a way, it reproduces the operator Ξ of Eq. (46) in Ref. [47].

In the end, one trades the potential-link interaction matrix element for a one-photon-exchange one,

$$\mathcal{V}_{ij} \rightarrow I_{iaja}(0), \quad (37)$$

to match the three-photon-exchange formulas. Let us pause and comment on the last step presented above. A link between the potential-like interaction and the one-photon-exchange interaction is drawn. The logic goes as follows; consider for example, the Wichmann-Kroll potential [49]. It accounts for an all-order treatment, in αZ , of the interaction of the free-electron vacuum-polarization loop (first order in α) with the

Coulomb potential [50]. (As a side comment, the Uehling potential [51], which takes into account the electric polarization of the vacuum (state), is the lowest order approximation (in αZ) of the vacuum-polarization loop within the Coulomb field of the nucleus. One usually considers that the Wichmann-Kroll potential does not take the Uehling potential into account.) Albeit the Wichmann-Kroll potential is such a potential-like interaction, it deals with the full Green's function. Though, the potential-like interaction considered above incorporates only the core electrons. Therefore, going half a step back, one can imagine to have an all-order αZ Wichmann-Kroll-like potential mapped to the vacuum-polarization loop only for the core electrons. The inner structure of the "vacuum-polarization potential-like" interaction is then unravelled by a cut in the loop. Hence, one can think of the potential-like interaction as an effective one-electron operator, but implicitly accounting for a corrected wave function or representing a screened correction.

Thus, one perturbs the S(VP)E equations (12)–(15) according to Eqs. (33–36) and finds the desired formulas under the

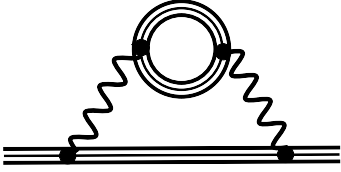


FIG. 4: One-particle two-loop Feynman diagram corresponding to the perturbed S(VP)P subset in the redefined vacuum state formalism in an external potential V . The triple line indicates the electron propagator perturbed by the potential-like interaction \mathcal{V} . Notation is similar to Fig. 2.

replacement (37). The Feynman diagram corresponding to the \mathcal{V} -perturbed S(VP)E subset is displayed in Fig. 4. The triple line notation represents the electron propagator perturbed by the potential-like interaction \mathcal{V} . It was shown that the two-electron subset and the three-electron subset are separately GI [25]. The perturbation is initially a potential-like interaction \mathcal{V} , turned into a one-photon-exchange operator in the vanishing energy limit, which is gauge independent too. Therefore, it should be well-founded to expect that the results derived from this approach also fulfill the requirement of gauge invariance, namely on the three- and four-electron level respectively. The open question is whether the separation into S(VP)EVP and S[V(VP)P]E subsets holds also at the three- and four-electron level, as it is thought to be the case. Hence, starting from the \mathcal{V} -perturbed S(VP)E GI expressions, one should be able to disentangle the various terms found via the redefinition of the vacuum state approach and assign them either to the three- or four-electron contribution. The results relying on this method are displayed in Appendix C for the former and in Appendix D for the latter.

V. REGULARIZATION OF INFRARED DIVERGENCES

Infrared divergences occur when the energy flowing through the loop (ω) leads to a vanishing denominator of the electron propagator at $\omega \rightarrow 0$. At the level of two-photon-exchange corrections, this behaviour was only met in ladder reducible expressions, where the removal of some terms in the summation of the crossed expressions was carried out to cancel IR divergent parts of the ladder reducible terms [52]. In the case of the three-photon-exchange corrections, it can also arise from crossed reducible expressions. The analysis of IR divergences is conducted in the Feynman gauge, but the resulting pairing of the expressions is valid generally in virtue

of gauge invariance. According to Shabaev [24], one introduces the following integral representation for the complex-exponential term of the photon propagator, including a photon mass term μ ,

$$e^{i\sqrt{\omega^2 - \mu^2 + i\varepsilon}|\mathbf{x} - \mathbf{y}|} = \frac{-2}{\pi} \int_0^\infty dk \frac{k \sin(k|\mathbf{x} - \mathbf{y}|)}{(\omega^2 - k^2 - \mu^2 + i\varepsilon)}. \quad (38)$$

The photon mass plays the role of a energy cutoff (IR regulator). Notice that the condition on the branch of the square root is changed to $\text{Im}(\sqrt{\omega^2 - \mu^2 + i\varepsilon}) > 0$. In the rest of the section, the use of $r_{12} \equiv |\mathbf{x} - \mathbf{y}|$ is preferred. Such type of integrals are met when facing IR divergences

$$\mathcal{I}_{n,m_\pm,p} \equiv \frac{-i}{2\pi} \int d\omega \frac{I(\omega)I(\omega)I(0)}{(-\omega + i\varepsilon)^n (\Delta \pm \omega + i\varepsilon)^m \tilde{\Delta}^p}, \quad (39)$$

with $n = 1, 2, 3$, $m = 0, 1$, $p = 0, 1$ and the constraint $n + m + p = 3$. The $+$ sign stands for the IR divergent ladder reducible terms and the $-$ sign for the compensating crossed terms. Calculations are performed by the application of #3.773(3) [or #3.729(2)] in Gradshteyn and Ryzhik [53]. The first step is to show that for a first-order pole, $n = 1$, the result is IR finite. There is no necessity to introduce a photon mass nor to use the integral representation of the complex exponential. It is sufficient to Wick rotate the integration contour with the substitution $\omega = i\omega_E$. Afterward, the principal value of the integral, denoted by \mathcal{P} , is considered. One shall start with the simplest case,

$$\begin{aligned} \mathcal{I}_{1,0,2} &= \frac{I(0)}{2\pi\tilde{\Delta}^2} \mathcal{P} \int_0^{i\infty} d\omega_E \frac{I(-i\omega_E)I(-i\omega_E) - I(i\omega_E)I(i\omega_E)}{i\omega_E} \\ &\quad - \frac{i}{2\tilde{\Delta}^2} I(0)I(0)I(0). \end{aligned} \quad (40)$$

The integral term reads explicitly

$$\frac{\alpha^2}{r_{12}r_{34}} \alpha_{1\mu} \alpha_2^\mu \alpha_{3\nu} \alpha_4^\nu \mathcal{P} \int_0^{i\infty} d\omega_E \frac{e^{-\omega_E R} - e^{\omega_E R}}{i\omega_E}, \quad (41)$$

giving a finite contribution in the limit $\omega \rightarrow 0$. R stands for $R = r_{12} + r_{34}$. One sees that the real part is IR finite, the imaginary one as well in this simple example. The second case, $\mathcal{I}_{1,2-,0}$, requires one more step, a partial fraction decomposition, so that the Cauchy principal value can be applied. Recall that the principal value picks only the residues, hence no contribution from second or higher order poles.

$$\begin{aligned} \mathcal{I}_{1,2-,0} &= \frac{I(0)}{2\pi\tilde{\Delta}^2} \mathcal{P} \int_0^{i\infty} d\omega_E \left\{ \frac{I(-i\omega_E)I(-i\omega_E) - I(i\omega_E)I(i\omega_E)}{i\omega_E} - \frac{I(-i\omega_E)I(-i\omega_E)}{\Delta + i\omega_E} - \frac{I(i\omega_E)I(i\omega_E)}{\Delta - i\omega_E} \right\} \\ &\quad - \frac{i}{\tilde{\Delta}^2} I(0) [I(0)I(0) - I(\Delta)I(\Delta)]. \end{aligned} \quad (42)$$

The first integrand was shown to IR finite just above. For the remaining two integrands, it is clear that Δ plays the role of an IR cutoff, preventing the expression to diverge in the limit $\omega \rightarrow 0$. The case $\mathcal{I}_{1,1-,1}$ is not met in the diagrams under consideration

and is therefore not assessed. Let us discuss the IR divergences arising from second-order poles. The first case, $\mathcal{I}_{2,0,1}$, considers the insertion of the interelectronic operator on the external leg of a one-loop diagram. One has,

$$\mathcal{I}_{2,0,1} = \frac{-\alpha^3 R}{\pi r_{12} r_{34} r_{56} \bar{\Delta}} \alpha_{1\mu} \alpha_2^\mu \alpha_{3\nu} \alpha_4^\nu \alpha_{5\rho} \alpha_6^\rho K_0(\mu R) \approx \frac{-\alpha^3 R}{\pi r_{12} r_{34} r_{56} \bar{\Delta}} \alpha_{1\mu} \alpha_2^\mu \alpha_{3\nu} \alpha_4^\nu \alpha_{5\rho} \alpha_6^\rho \left(\ln \frac{\mu}{2} + \gamma + \ln R \right), \quad (43)$$

in the limit $\mu \rightarrow 0$. $K_n(x)$ are imaginary Bessel functions of the second kind. The identical IR logarithmic divergent behaviour as in the two-photon-exchange ladder reducible case is recovered [24]. The corresponding crossed diagram cancels the IR divergent term, leaving a well-behaved expression. The second case, $\mathcal{I}_{2,1+,0}$, is when the interelectronic operator is inserted within the electron propagator of the loop in the diagram. One faces

$$\mathcal{I}_{2,1+,0} = \frac{\alpha^3}{\pi r_{12} r_{34} r_{56}} \alpha_{1\mu} \alpha_2^\mu \alpha_{3\nu} \alpha_4^\nu \alpha_{5\rho} \alpha_6^\rho \int_0^\infty dk k \sin(kR) \left[\frac{1}{(k^2 + \mu^2)^{3/2} (\Delta - \sqrt{k^2 + \mu^2})} - \frac{2}{(k^2 + \mu^2) \Delta^2} \right]. \quad (44)$$

This IR divergence is compensated by a similar crossed graph, represented by the intergral $\mathcal{I}_{2,1-,0}$ where the interelectronic operator is also inserted within the electron propagator of the loop

$$\begin{aligned} \mathcal{I}_{2,1-,0} &= \frac{-\alpha^3}{\pi r_{12} r_{34} r_{56}} \alpha_{1\mu} \alpha_2^\mu \alpha_{3\nu} \alpha_4^\nu \alpha_{5\rho} \alpha_6^\rho \int_0^\infty dk k \sin(kR) \\ &\times \left[\frac{-1}{(k^2 + \mu^2)^{3/2} (\Delta + \sqrt{k^2 + \mu^2})} + \frac{2}{(k^2 + \mu^2 - \Delta^2) \Delta^2} - \frac{2}{(k^2 + \mu^2) \Delta^2} \right]. \end{aligned} \quad (45)$$

However, the cancellation is not straightforward at this step. A partial fraction decomposition allows to greatly simplify the previous expressions, when they are added together.

$$\begin{aligned} \mathcal{I}_{2,1-,0} + \mathcal{I}_{2,1+,0} &= \frac{-2\alpha^3}{\pi r_{12} r_{34} r_{56} \Delta^2} \alpha_{1\mu} \alpha_2^\mu \alpha_{3\nu} \alpha_4^\nu \alpha_{5\rho} \alpha_6^\rho \int_0^\infty dk \frac{k \sin(kR)}{k^2 + \mu^2} \\ &= \frac{-2\alpha^3}{\pi r_{12} r_{34} r_{56} \Delta^2} \alpha_{1\mu} \alpha_2^\mu \alpha_{3\nu} \alpha_4^\nu \alpha_{5\rho} \alpha_6^\rho \sqrt{\frac{\pi \mu R}{2}} K_{1/2}(\mu R) \approx \frac{\alpha^3}{r_{12} r_{34} r_{56} \Delta^2} \alpha_{1\mu} \alpha_2^\mu \alpha_{3\nu} \alpha_4^\nu \alpha_{5\rho} \alpha_6^\rho (\mu R - 1). \end{aligned} \quad (46)$$

Thus, it turned out to be a spurious divergence; the IR divergence is ruled out and a finite part remains in the limit $\mu \rightarrow 0$. Last, but not least, the IR divergence arising from the third-order pole is treated. The corresponding integral to evaluate is

$$\mathcal{I}_{3,0,0} = \frac{-\alpha^3}{\pi r_{12} r_{34} r_{56}} \alpha_{1\mu} \alpha_2^\mu \alpha_{3\nu} \alpha_4^\nu \alpha_{5\rho} \alpha_6^\rho \sqrt{\frac{\pi R}{2\mu}} \frac{R}{2} K_{1/2}(\mu R) \approx \frac{-\alpha^3 R}{4r_{12} r_{34} r_{56}} \alpha_{1\mu} \alpha_2^\mu \alpha_{3\nu} \alpha_4^\nu \alpha_{5\rho} \alpha_6^\rho \left(\frac{1}{\mu} - R \right), \quad (47)$$

leading to a singular behaviour when the limit $\mu \rightarrow 0$ is taken. The behaviour of the IR divergence arising from the third-order pole is in agreement with the one presented in Ref. [48], where a similar analysis was performed for the self-energy screening effects in g -factor calculations. A different treatment for the regularization of the IR divergence for the third-order pole based on a symmetry argument is proposed in Appendix E. Similarly to the IR divergence arising from the second-order pole, one looks for the compensating crossed diagram to ensure that the total expression is finite.

The explicit cancellation of IR divergences, at the individual Feynman diagram level by the appropriate crossed term, is demonstrated in Table I. An exception is met for the ladder reducible 2 terms, which compensate themselves. A swapping of the indices in the expressions presented in Section III might be sometimes necessary in order to make the compensation apparent. Moreover, it was shown that IR divergences

are absorbed by expressions belonging to the same subset.

VI. COMPARISON

Two different approaches were utilized to infer a partial third-order interelectronic correction to the energy shift. A comparison between the results of each of these two approaches is undertaken in this section.

The discussion begins with the four-electron contribution, which involves three types of terms: the irreducible $[\Delta E_v^{(3I)4e,irr}$ (D1, D2)], the reducible 1 $[\Delta E_v^{(3I)4e,red1}$ (D3, D4)] and the reducible 2 $[\Delta E_v^{(3I)4e,red2}$ (D5, D6)]. For every type previously stated, agreement between the perturbative treatment of the \mathcal{V} -perturbed S(VP)E three-electron subset and the effective one-particle approach is met.

For the three-electron contribution, an identical separation

TABLE I: IR divergences regularization at the individual Feynman diagram level. IR divergences are found in the reducible expressions, both for ladder- and crossed-loops. Crossed stands for the crossed compensating term. $\mathcal{I}_{n,m_{\pm},p}$ describes the type of divergent integral encountered in the graph. Each term can be found in Chapter. III, following the referenced equation. The labels are simplified in comparison to the ones presented there, only the difference among them is highlighted.

$\Delta E_v^{(31)3e} \in S[V(VP)P]E$	type of IR divergence	Crossed	IR compensation
H_1 : ladder red 1 (23)	$\mathcal{I}_{2,1+,0}$	H_2 : crossed (A1)	$\mathcal{I}_{2,1-,0}$
H_1 : ladder red 1(24)	$\mathcal{I}_{2,1+,0}$	H_2 : crossed (A1)	$\mathcal{I}_{2,1-,0}$
H_1 : ladder red 2 (25)	$\mathcal{I}_{3,0,0}$	H_2 : ladder red 2 (A7)	$\mathcal{I}_{3,0,0}$
H_1 : crossed red (26)	$\mathcal{I}_{2,1-,0}, \mathcal{I}_{3,0,0}$	H_2 : crossed (A1)	$\mathcal{I}_{2,1-,0}, \mathcal{I}_{3,0,0}$
H_2 : ladder red 1 (A3)	$\mathcal{I}_{2,0,1}$	H_1 : crossed irr (21)	$\mathcal{I}_{2,0,1}$
H_2 : ladder red 1 (A5)	$\mathcal{I}_{2,0,1}$	H_1 : crossed irr (20)	$\mathcal{I}_{2,0,1}$
H_2 : ladder red 2 (A7)	$\mathcal{I}_{3,0,0}$	H_1 : ladder red 2 (25)	$\mathcal{I}_{3,0,0}$
$\Delta E_v^{(31)3e} \in S(VP)EVP$	type of IR divergence	Crossed	IR compensation
F_1 : ladder red 1 (B7)	$\mathcal{I}_{2,0,1}$	F_1 : crossed (B3)	$\mathcal{I}_{2,0,1}$
F_2 : ladder red 1(30)	$\mathcal{I}_{2,1+,0}$	F_2 : crossed (28)	$\mathcal{I}_{2,1-,0}$
F_2 : ladder red 1 (31)	$\mathcal{I}_{2,1+,0}$	F_2 : crossed (28)	$\mathcal{I}_{2,1-,0}$
F_2 : ladder red 2 (32)	$\mathcal{I}_{3,0,0}$	F_2 : crossed (28)	$\mathcal{I}_{3,0,0}$
F_3 : ladder red 1 (B14)	$\mathcal{I}_{2,0,1}$	F_3 : crossed irr (B10)	$\mathcal{I}_{2,0,1}$
F_3 : ladder red 2 (B15)	$\mathcal{I}_{3,0,0}$	F_3 : crossed red (B11)	$\mathcal{I}_{3,0,0}$
F_3 : crossed red (B11)	$\mathcal{I}_{2,1-,0}$	F_2 : crossed (28)	$\mathcal{I}_{2,1-,0}$

as above is conducted. The irreducible type is composed of three parts, two of which correspond to crossed diagrams, $[\Delta E_v^{(31)3e,cross} (C4,C5), \Delta E_v^{(31)3e,cross,irr} (C2, C3)]$ and one corresponding to ladder diagrams $[\Delta E_v^{(31)3e,lad,irr} (C6, C7)]$. The outcomes of the two methods are in full concordance for these terms. Regarding the reducible 1 type, the cross reducible $[\Delta E_v^{(31)3e,cross,red} (C8, C9)]$ and the ladder reducible 1 IR free ω $[\Delta E_v^{(31)lad,red1} (C14, C15)]$ terms extracted from the two treatments are in good agreement.

However, for the remaining reducible 1 terms $[\Delta E_v^{(31)3e,lad,red1} (C10, C11), \Delta E_v^{(31)3e,lad,red1} (C12, C13)]$ a discrepancy is encountered. Yerokhin, in Ref. [47], already pointed out that the perturbation theory approach runs into troubles to deal with reducible terms (See remarks below Eqs. (32, 35, 37) in Ref. [47]). He is invoking gauge invariance to fix the problem. If proceeding as explained at the beginning of the section dedicated to perturbation theory approach, an identical problem to the one highlighted by Yerokhin is met, namely that the poles differ by the sign of the $i\epsilon$ prescription,

$$\frac{1}{(\omega + i\epsilon)(-\omega + i\epsilon)} \quad \text{versus} \quad \frac{1}{(\omega + i\epsilon)^2} \quad \text{or} \quad \frac{1}{(-\omega + i\epsilon)^2}, \quad (48)$$

when facing ladder reducible 1 terms, $\Delta E_v^{(31)3e,lad,red1}$ and $\Delta E_v^{(31)3e,lad,red1}$. The difference in the topology of the poles arises from unaccounted restrictions in the summations. Surprisingly, and possibly related to the topology problem associated with the poles, the two approaches differ regarding the

extra terms

$$\Delta E_{v, S[V(VP)P]E}^{(31)3e,red1} = \sum_{a,b,b_1,v_1,i}^{i \neq v} \frac{I_{vbb_1v_1}(\Delta_{vb})I_{v_1aia}(0)I_{ib_1bv}(\Delta_{vb})}{(\epsilon_v - \epsilon_i)^2}, \quad (49)$$

and

$$\Delta E_{v, S(VP)EVP}^{(31)3e,red1} = - \sum_{a,b,b_1,v_1,i}^{i \neq b} \frac{I_{vbb_1v_1}(\Delta_{vb})I_{b_1aia}(0)I_{iv_1vb}(\Delta_{vb})}{(\epsilon_b - \epsilon_i)^2}. \quad (50)$$

These are not found via the perturbative analysis but are present in the redefined vacuum state approach. They are obtained as the interplay among terms generated from the ladder reducible 1 terms, upon the symmetrisation of the energy flow in the loop, and four-electron reducible 1 terms. The former originates from H_1 while the latter originates from F_2 . They look like four-electron reducible 1 contribution, due to the absence of the ω integration. According to the gauge invariance of the three-electron S(VP)E subset of the two-photon-exchange corrections, they should be incorporated in the three-electron contribution of the three-photon-exchange corrections. The structure of these terms suggests them to be included in the reducible 1 contribution. The last point to be made concerning these two terms is that they are obviously IR finite.

The reducible 2 type contains only ladder reducible 2 terms, the IR free one $[\Delta E_v^{(31)3e,lad,red2} (C18, C19)]$, and the IR di-

vergent one $[\Delta E_{v, \text{IR div}}^{(31)3e, \text{lad, red2}}]$ (C16, C17)]. The expressions obtained from the two different methods are identical.

Overall, if errors occurred in the different three-electron types of interelectronic interactions considered, one would expect to see repercussions in the four-electron contribution. In this case, the four-electron contribution would suffer from discrepancies between the two methods, a behaviour which is not encountered. Therefore, these two independent derivations and the comparison of the resulting expressions presented in the present work are fully consistent, except for two expressions mentioned above. In these cases, the discrepancy can be traced back to unaccounted restrictions in the summations, resulting in a different topology of the poles. Furthermore, the derivation based on this two-method scheme is a good sanity check of the obtained formulas. The perturbation theory approach also helped to sort out the three- and four-electron contributions, especially for the extra terms given in Eqs. (49, 50). In summary, the gathered evidences point towards the consistency of the derived three-electron expressions. Moreover, the excellent agreement met at the four-electron contribution level serves as a strong indication that the three-electron expressions should be reliable.

Concerning the separation into the proposed GI subsets, S[V(VP)P]E and S(VP)EVP, the cancellation of IR divergences by elements from the same subset is very assuring. A numerical evaluation of the derived expressions is the sole way to either affirm the conjectured separability into the GI subsets put forward here, based on analytical considerations, or to confirm it and therewith turn it into a solid claim.

VII. DISCUSSION AND CONCLUSION

The expressions presented in the work can readily be applied to any Li-like and/or B-like atoms or ions. They represent an important first step toward the evaluation of third-order interelectronic interactions. The three-photon-exchange formulas were explicitly derived for two proposed GI subsets arising from two classes of one-particle three-loop Feynman diagrams. The derivation relies on an effective one-particle approach, owing to the redefinition of the vacuum state, in the framework of the TTGF method. The resulting formulas contained infrared divergences. They were investigated and regularized by the introduction of a photon mass term. Two different types of divergences were encountered when the photon mass is sent to zero: a logarithmic one (43) and a first-order singular one (47). The divergent behaviours observed are in full accordance with previous studies [24, 48]. In order to allow for a verification of the expressions derived in the framework of the TTGF, an independent derivation was conducted with the help of perturbation theory. However, from the very beginning of the study, the issue of the topology of the pole was known for the second method; see the detailed explanation in the work of Yerokhin *et al.* [47]. Nevertheless, the idea of the present work was to see how far one can get with the cross-check, relying on the possibility of a perturbative treatment. This helped to resolve the different reducible terms (red1 and red2) and to sort out the distribution of different con-

tributions (three-electron and four-electron) in each expression of the subsets (S[V(VP)P]E and S(VP)EVP). The agreement between the two approaches, at the four-electron level, is excellent. At the three-electron level, a reasonable agreement is met between the two results. Here, the discrepancy related to the different topology of the poles encountered in the (three-electron) ladder reducible 1 terms, for both IR divergent and IR finite ones, prevents to achieve a complete agreement. The difference in the topology of the poles could be attributed to unaccounted restrictions in summations. In fact such discrepancy in the topology of the poles was already encountered when comparing the results for the two-photon-exchange contributions between Refs. [22, 54] and Ref. [25]. The comparison between the results for the two-photon-exchange two-electron contributions showed that the difference in the topology of the poles did not affect significantly the numerical values; the difference amounts to $\mathcal{O}(7 \cdot 10^{-4})$ atomic unit, or $\mathcal{O}(1.9 \cdot 10^{-2})$ eV. An open question lies in the fact if the extra terms are related to this issue, and if the role they are playing potentially is to ensure gauge invariance.

Based on the intuition acquired within the perturbative treatment, we do believe that the strong constraint of gauge invariance can be tracked to the third-order as well. Hence, it should be well-based to expect that the results derived from this approach also fulfill the requirement of gauge invariance. Thus, in analogy to the perturbation theory approach, our belief is that the outcome of the TTGF method is also characterized by the important paradigm of gauge invariance. Whether a further separation according to the subsets is possible cannot be resolved yet. Nevertheless, from the TTGF perspective, the explicit cancellation of IR divergences, within each subset, is very engaging. Last, but not least, a successful verification of the derived expressions was also carried out for the three-electron contribution with the g -factor formulas derived in Ref. [30], under the replacement (37). Note that the extra terms are also present in those formulas; they manifest themselves when one proceeds towards numerical evaluations [55].

To conclude, the method based on a vacuum state redefinition in QED has shown, in this work, to be a well-suited tool to perform elaborate calculations. In contrast to other methods, it permits the identification of GI subsets and inherently, thus, validates the consistency of the obtained results. This asset can be very useful in future derivations of higher-order contributions since it provides a robust verification. Developing on this intrinsic characteristic, and to highlight the possibility to apply the formalism for advanced calculations, an investigation of third-order interelectronic corrections was carried out. Moreover, the identification of GI expressions within this approach paves the way for calculating higher-order corrections, which can be split into GI subsets and tackled one after the other. The presented redefined vacuum state approach can be further employed for atoms with a (more) sophisticated electronic structure, as it allows to focus only on the particles that differentiate between the configurations.

VIII. ACKNOWLEDGMENTS

This work is supported by Bundesministerium für Bildung und Forschung (BMBF) through project 05P21SJFAA. R.N.S.

is grateful to A. V. Volotka for helpful discussions, and to F. Karbstein for his help in improving the quality of the manuscript and its readability.

Appendix A: Three-electron terms arising from the H_2 diagram

The expressions extracted from the H_2 Feynman diagram are found as follows,

$$\Delta E_{v, H_2}^{(3I)3e, \text{cross}} = \frac{i}{2\pi} \int d\omega \sum_{i,j,k} \frac{I_{vji}(\omega) I_{kaja}(0) I_{bikv}(\omega)}{(\epsilon_v - \omega - \epsilon_i u)(\epsilon_b - \omega - \epsilon_j u)(\epsilon_b - \omega - \epsilon_k u)}, \quad (\text{A1})$$

$$\Delta E_{v, H_2}^{(3I)3e, \text{lad, irr}} = \frac{i}{2\pi} \int d\omega \sum_{i,j,k}^{k \neq b, \{i,j\} \neq \{b,v\}} \frac{I_{vbj}(\omega) I_{kaba}(0) I_{jikv}(\omega)}{(\epsilon_v - \omega - \epsilon_i u)(\epsilon_b + \omega - \epsilon_j u)(\epsilon_b - \epsilon_k u)}, \quad (\text{A2})$$

$$\Delta E_{v, H_2}^{(3I)3e, \text{lad, red1}} = -\frac{i}{2\pi} \int d\omega \sum_{i,j,k}^{k \neq b, \{i,j\} = \{b,v\}} \frac{I_{vbj}(\omega) I_{kaba}(0) I_{jikv}(\omega)}{(\epsilon_v - \omega - \epsilon_i u)^2 (\epsilon_b - \epsilon_k u)}, \quad (\text{A3})$$

$$\Delta E_{v, H_2}^{(3I)3e, \text{lad, irr}} = \frac{i}{2\pi} \int d\omega \sum_{i,j,k}^{k \neq b, \{i,j\} \neq \{b,v\}} \frac{I_{vki}(\omega) I_{baka}(0) I_{jibv}(\omega)}{(\epsilon_v - \omega - \epsilon_i u)(\epsilon_b + \omega - \epsilon_j u)(\epsilon_b - \epsilon_k u)}, \quad (\text{A4})$$

$$\Delta E_{v, H_2}^{(3I) \text{lad, red1}} = -\frac{i}{2\pi} \int d\omega \sum_{i,j,k}^{k \neq b, \{i,j\} = \{b,v\}} \frac{I_{vki}(\omega) I_{baka}(0) I_{jibv}(\omega)}{(\epsilon_v - \omega - \epsilon_i u)^2 (\epsilon_b - \epsilon_k u)}. \quad (\text{A5})$$

The non-diagrammatic term for H_2 are found to be

$$\Delta E_{v, H_2}^{(3I)3e, \text{lad, red1}} = -\frac{i}{2\pi} \int d\omega \sum_{i,j}^{\{i,j\} \neq \{b,v\}} \frac{I_{vbj}(\omega) I_{b1aba}(0) I_{jib1v}(\omega)}{(\epsilon_v - \omega - \epsilon_i u)(\epsilon_b + \omega - \epsilon_j u)^2}, \quad (\text{A6})$$

$$\Delta E_{v, H_2}^{(3I)3e, \text{lad, red2}} = -\frac{i}{2\pi} \int d\omega \sum_{i,j}^{\{i,j\} = \{b,v\}} \frac{I_{vbj}(\omega) I_{b1aba}(0) I_{jib1v}(\omega)}{(\epsilon_v - \omega - \epsilon_i u)^3}. \quad (\text{A7})$$

Appendix B: Three-electron terms arising from the F_1 and F_3 diagrams

Within this subset, the Green's function associated to the remaining diagrams reads

$$\begin{aligned} \Delta g_{\alpha, vv}^{(3)F_1}(E) &= \frac{1}{(E - \epsilon_v)^2} \left(\frac{i}{2\pi} \right)^3 \sum_{i,j,k,l,p} \int d\omega dk_1 dk_2 \frac{I_{viji}(0)}{[k_1 - \epsilon_i + i\varepsilon(\epsilon_i - E_\alpha^F)][E - \epsilon_j + i\varepsilon(\epsilon_j - E_\alpha^F)]} \\ &\times \frac{I_{jpk}(\omega) I_{klvp}(\omega)}{[E - \omega - \epsilon_k + i\varepsilon(\epsilon_k - E_\alpha^F)][k_2 - \epsilon_l + i\varepsilon(\epsilon_l - E_\alpha^F)][k_2 - \omega - \epsilon_p + i\varepsilon(\epsilon_p - E_\alpha^F)]}, \end{aligned} \quad (\text{B1})$$

for F_1 , and

$$\begin{aligned} \Delta g_{\alpha, vv}^{(3)F_3}(E) &= \frac{1}{(E - \epsilon_v)^2} \left(\frac{i}{2\pi} \right)^3 \sum_{i,j,k,l,p} \int d\omega dk_1 dk_2 \frac{I_{vki}(\omega)}{[E - \omega - \epsilon_i + i\varepsilon(\epsilon_i - E_\alpha^F)][k_1 - \epsilon_j + i\varepsilon(\epsilon_j - E_\alpha^F)]} \\ &\times \frac{I_{ijlk}(\omega) I_{lpvp}(0)}{[k_1 - \omega - \epsilon_k + i\varepsilon(\epsilon_k - E_\alpha^F)][E - \epsilon_l + i\varepsilon(\epsilon_l - E_\alpha^F)][k_2 - \epsilon_p + i\varepsilon(\epsilon_p - E_\alpha^F)]}. \end{aligned} \quad (\text{B2})$$

for F_3 . The extraction procedure is carried out for the F_1 Feynman diagram, which contributes as follow. The terms associated to the crossed graphs are

$$\Delta E_{v, F_1}^{(3I)3e, \text{cross}, \text{irr}} = \frac{i}{2\pi} \int d\omega \sum_{i,j,k}^{i \neq v} \frac{I_{vaia}(0) I_{ikjb}(\omega) I_{bjkv}(\omega)}{(\epsilon_v - \epsilon_i)(\epsilon_v - \omega - \epsilon_j u)(\epsilon_b - \omega - \epsilon_k u)}, \quad (\text{B3})$$

$$\Delta E_{v, F_1}^{(3I)3e, \text{cross}, \text{red1}} = -\frac{i}{2\pi} \int d\omega \sum_{i,j} \frac{I_{vav_1a}(0) I_{v_1kjb}(\omega) I_{bjkv}(\omega)}{(\epsilon_v - \omega - \epsilon_j u)^2 (\epsilon_b - \omega - \epsilon_k u)}. \quad (\text{B4})$$

The expressions corresponding to the ladder-loop graph read

$$\Delta E_{v, F_1}^{(3I)3e, \text{ladder}, \text{irr}} = \frac{i}{2\pi} \int d\omega \sum_{i,j,k}^{i \neq v, \{j,k\} \neq \{v,b\}} \frac{I_{vaia}(0) I_{ibjk}(\omega) I_{jkvb}(\omega)}{(\epsilon_v - \epsilon_i u)(\epsilon_v - \omega - \epsilon_j u)(\epsilon_b + \omega - \epsilon_k u)}, \quad (\text{B5})$$

$$\Delta E_{v, F_1}^{(3I)3e, \text{ladder}, \text{red1}} = -\frac{i}{2\pi} \int d\omega \sum_{i,j,k}^{\{j,k\} \neq \{v,b\}} \frac{I_{vav_1a}(0) I_{v_1bjk}(\omega) I_{jkvb}(\omega)}{(\epsilon_v - \omega - \epsilon_j u)^2 (\epsilon_b + \omega - \epsilon_k u)}, \quad (\text{B6})$$

$$\begin{aligned} \Delta E_{v, F_1}^{(3I)3e, \text{ladder}, \text{red1}} = & -\frac{i}{2\pi} \int d\omega \sum_{i,j,k}^{i \neq v, \{j,k\} = \{v,b\}} \left\{ \frac{I_{vaia}(0) I_{ibjk}(\omega) I_{jkvb}(\omega)}{(\epsilon_v - \epsilon_i u)^2} \left[\frac{1}{(\epsilon_v - \omega - \epsilon_j u)} + \frac{1}{(\epsilon_b + \omega - \epsilon_k u)} \right] \right. \\ & \left. + \frac{I_{vaia}(0) I_{ibjk}(\omega) I_{jkvb}(\omega)}{(\epsilon_v - \epsilon_i u)(\epsilon_v - \omega - \epsilon_j u)^2} \right\}, \quad (\text{B7}) \end{aligned}$$

$$\Delta E_{v, F_1}^{(3I)3e, \text{ladder}, \text{red2}} = \frac{i}{2\pi} \int d\omega \sum_{j,k}^{\{j,k\} = \{v,b\}} \frac{I_{vav_1a}(0) I_{v_1bjk}(\omega) I_{jkvb}(\omega)}{(\epsilon_v - \omega - \epsilon_j u)^3}. \quad (\text{B8})$$

For the disconnected parts, the terms presented below cancel the reducible elements found in F_1 , namely the term on the first line cancels (B4), the term in the second line cancels (B6) and the term in the third line cancels (B8). It leaves only the irreducible expressions and the ladder reducible 1 term (B7).

$$\begin{aligned} \Delta E_{v, F}^{(3I)3e, \text{disc}} = & \frac{i}{2\pi} \int d\omega \left\{ \sum_{i,j} \frac{I_{vava}(0) I_{v_1jib}(\omega) I_{ibv_1j}(\omega)}{(\epsilon_v - \omega - \epsilon_i u)^2 (\epsilon_b - \omega - \epsilon_j u)} + \sum_{i,j}^{\{i,j\} \neq \{b,v\}} \frac{I_{vava}(0) I_{v_1bij}(\omega) I_{ijv_1bj}(\omega)}{(\epsilon_v - \omega - \epsilon_i u)^2 (\epsilon_b + \omega - \epsilon_j u)} \right. \\ & \left. - \sum_{i,j}^{\{i,j\} = \{b,v\}} \frac{I_{vava}(0) I_{v_1bij}(\omega) I_{ijv_1bj}(\omega)}{(\epsilon_v - \omega - \epsilon_i u)^3} \right\}. \quad (\text{B9}) \end{aligned}$$

From the F_3 Feynman diagram arises the following terms. Similarly to the F_1 graph, the terms corresponding to the crossed graph are

$$\Delta E_{v, F_3}^{(3I)3e, \text{cross}, \text{irr}} = \frac{i}{2\pi} \int d\omega \sum_{i,j,k}^{k \neq v} \frac{I_{vjib}(\omega) I_{ibkj}(\omega) I_{kava}(0)}{(\epsilon_v - \omega - \epsilon_i u)(\epsilon_b - \omega - \epsilon_j u)(\epsilon_v - \epsilon_k u)}, \quad (\text{B10})$$

$$\Delta E_{v, F_3}^{(3I)3e, \text{cross}, \text{red}} = \frac{-i}{2\pi} \int d\omega \sum_{i,j} \frac{I_{vjib}(\omega) I_{ibv_1j}(\omega) I_{v_1ava}(0)}{(\epsilon_v - \omega - \epsilon_i u)^2 (\epsilon_b - \omega - \epsilon_j u)}. \quad (\text{B11})$$

The ones associated to the ladder graph read

$$\Delta E_{v, F_3}^{(3I)3e, \text{ladder}, \text{irr}} = \frac{i}{2\pi} \int d\omega \sum_{i,j,k}^{\{i,j\} \neq \{b,v\}, k \neq v} \frac{I_{vbij}(\omega) I_{ijkb}(\omega) I_{kava}(0)}{(\epsilon_v - \omega - \epsilon_i u)(\epsilon_b + \omega - \epsilon_j u)(\epsilon_v - \epsilon_k u)}, \quad (\text{B12})$$

$$\Delta E_{v, F_3}^{(3l)lad, red1} = \frac{-i}{2\pi} \int d\omega \sum_{i,j}^{\{i,j\} \neq \{b,v\}} \frac{I_{vbj}(\omega) I_{ijv_1b}(\omega) I_{v_1ava}(0)}{(\epsilon_v - \omega - \epsilon_i u)^2 (\epsilon_b + \omega - \epsilon_j u)}, \quad (B13)$$

$$\begin{aligned} \Delta E_{v, F_3}^{(3l)3e, lad, red1} &= \frac{-i}{2\pi} \int d\omega \sum_{i,j,k}^{\{i,j\} = \{b,v\}, k \neq v} \left\{ \frac{I_{vbj}(\omega) I_{ijkb}(\omega) I_{kava}(0)}{(\epsilon_v - \epsilon_k u)^2} \left[\frac{1}{(\epsilon_v - \omega - \epsilon_i u)} + \frac{1}{(\epsilon_b + \omega - \epsilon_j u)} \right] \right. \\ &\quad \left. + \frac{I_{vbj}(\omega) I_{ijkb}(\omega) I_{kava}(0)}{(\epsilon_v - \omega - \epsilon_i u)^2 (\epsilon_v - \epsilon_k u)} \right\}, \end{aligned} \quad (B14)$$

$$\Delta E_{v, F_3}^{(3l)3e, lad, red2} = \frac{i}{2\pi} \int d\omega \sum_{i,j}^{\{i,j\} = \{b,v\}} \frac{I_{vbj}(\omega) I_{ijv_1b}(\omega) I_{v_1ava}(0)}{(\epsilon_v - \omega - \epsilon_i u)^3}. \quad (B15)$$

Appendix C: Third-order interelectronic corrections derived by a perturbative treatment: three-electron subset

The idea would be to proceed as follows; one perturbs the S(VP)E two-electron expressions (12, 13) according to Eqs. (33–36) and finds the desired formulas under the replacement (37). However, the issue is, as already pointed out by Yerokhin in Ref. [47], that this approach suffers from troubles to deal with reducible terms [63]. He is invoking gauge invariance to fix the problem. If proceeding as explained just above, an identical problem to the one highlighted by Yerokhin is met, namely that the poles differ by the sign of the $i\varepsilon$ prescription [64],

$$\frac{1}{(\omega + i\varepsilon)(-\omega + i\varepsilon)} \quad \text{versus} \quad \frac{1}{(\omega + i\varepsilon)^2} \quad \text{or} \quad \frac{1}{(-\omega + i\varepsilon)^2}, \quad (C1)$$

when facing ladder reducible 1 contributions, $\Delta E_{v, IR \text{ div}}^{(3l)3e, lad, red1}$ and $\Delta E_{v, IR \text{ free}}^{(3l)3e, lad, red1}$. The difference in the topology of the poles arises from unaccounted restrictions in the summations. Nevertheless, for the sake of the verification, it is worth tackling this perturbative analysis and see how far one can get. However, due to this previous discrepancy, the different three-electron terms presented below are those derived within the redefinition of the vacuum state formalism. They are separated into irreducible (irr), reducible 1 (red1) and reducible 2 (red2) types, and moreover into S[V(VP)P]E and S(VP)EVP according to their originated diagrams.

1. Irreducible terms

The crossed irreducible expression, a new feature showing up at this order, is presented first. A separation according to the belonging to each subset is conducted,

$$\Delta E_{v, S[V(VP)P]E}^{(3l)3e, cross, irr} = \frac{i}{2\pi} \int d\omega \sum_{a,b,i,j,k}^{k \neq b} \frac{I_{vjib}(\omega) I_{baka}(0) I_{ikvj}(\omega) + I_{vjik}(\omega) I_{kaba}(0) I_{ibvj}(\omega)}{(\epsilon_v - \omega - \epsilon_i u)(\epsilon_b - \omega - \epsilon_j u) \Delta_{bk}}, \quad (C2)$$

$$\Delta E_{v, S(VP)EVP}^{(3l)3e, cross, irr} = \frac{i}{2\pi} \int d\omega \sum_{a,b,i,j,k}^{i \neq v} \frac{I_{vaia}(0) I_{ikjb}(\omega) I_{bjkv}(\omega) + I_{vkjb}(\omega) I_{jbik}(\omega) I_{aia v}(0)}{\Delta_{vi}(\epsilon_v - \omega - \epsilon_j u)(\epsilon_b - \omega - \epsilon_k u)}. \quad (C3)$$

Then, the crossed expression, also separated according to their origin diagrams, is displayed,

$$\Delta E_{v, S[V(VP)P]E}^{(3l)3e, cross} = \frac{i}{2\pi} \int d\omega \sum_{a,b,i,j,k} \frac{I_{vjib}(\omega) I_{akaj}(0) I_{ibvk}(\omega)}{(\epsilon_v - \omega - \epsilon_i u)(\epsilon_b - \omega - \epsilon_j u)(\epsilon_b - \omega - \epsilon_k u)} \quad (C4)$$

$$\Delta E_{v, S(VP)EVP}^{(3l)3e, cross} = \frac{i}{2\pi} \int d\omega \sum_{a,b,i,j,k} \frac{I_{vkib}(\omega) I_{ajia}(0) I_{bjkv}(\omega)}{(\epsilon_v - \omega - \epsilon_i u)(\epsilon_v - \omega - \epsilon_j u)(\epsilon_b - \omega - \epsilon_k u)}. \quad (C5)$$

Finally, the ladder irreducible expression is found as

$$\begin{aligned} \Delta E_{v, S[V(VP)P]E}^{(3I)3e,lad,irr} = & \frac{i}{2\pi} \int d\omega \left[\sum_{a,b,i,j,k}^{k \neq b, \{i,j\} \neq \{v,b\}} \frac{I_{vbij}(\omega) I_{akab}(0) I_{ijvk}(\omega) + I_{vki j}(\omega) I_{abak}(0) I_{ijvb}(\omega)}{(\epsilon_v - \omega - \epsilon_i u)(\epsilon_b + \omega - \epsilon_j u) \Delta_{bk}} \right. \\ & \left. + \sum_{a,b,i,j,k}^{\{i,j\} \neq \{v,b\}, \{i,k\} \neq \{v,b\}} \frac{I_{vbij}(\omega) I_{jaka}(0) I_{ikvb}(\omega)}{(\epsilon_v - \omega - \epsilon_i u)(\epsilon_b + \omega - \epsilon_j u)(\epsilon_b + \omega - \epsilon_k u)} \right], \end{aligned} \quad (C6)$$

$$\begin{aligned} \Delta E_{v, S(VP)EVP}^{(3I)3e,lad,irr} = & \frac{i}{2\pi} \int d\omega \left[\sum_{a,b,i,j,k}^{i \neq v, \{j,k\} \neq \{v,b\}} \frac{I_{vaia}(0) I_{ibjk}(\omega) I_{kjbv}(\omega) + I_{vbjk}(\omega) I_{jkib}(\omega) I_{aiav}(0)}{\Delta_{vi}(\epsilon_v - \omega - \epsilon_j u)(\epsilon_b + \omega - \epsilon_k u)} \right. \\ & \left. + \sum_{a,b,i,j,k}^{\{i,k\} \neq \{v,b\}, \{j,k\} \neq \{v,b\}} \frac{I_{vbik}(\omega) I_{iaja}(0) I_{kjbv}(\omega)}{(\epsilon_v - \omega - \epsilon_i u)(\epsilon_v - \omega - \epsilon_j u)(\epsilon_b + \omega - \epsilon_k u)} \right]. \end{aligned} \quad (C7)$$

2. Reducible 1 terms

Since a crossed irreducible expression exist, the associated crossed reducible terms are found and worked out. The result is separated as well according to the originated subset, and reads

$$\Delta E_{v, S[V(VP)P]E}^{(3I)3e,cross,red} = -\frac{i}{2\pi} \int d\omega \sum_{a,b,b_1,i,j} \frac{I_{vjib}(\omega) I_{bab_1a}(0) I_{ib_1vj}(\omega)}{(\epsilon_v - \omega - \epsilon_i u)(\epsilon_b - \omega - \epsilon_j u)^2}, \quad (C8)$$

$$\Delta E_{v, S(VP)EVP}^{(3I)3e,cross,red} = -\frac{i}{2\pi} \int d\omega \sum_{a,b,v_1,i,j} \frac{I_{vjib}(\omega) I_{bijv_1}(\omega) I_{av_1av}(0)}{(\epsilon_v - \omega - \epsilon_i u)^2(\epsilon_b - \omega - \epsilon_j u)}. \quad (C9)$$

Each ladder reducible 1 term is separated into an IR free and an IR divergent part, and displayed according to its provenance. Beginning with the latter, one has

$$\begin{aligned} \Delta E_{v, S[V(VP)P]E, IR \text{ div}}^{(3I)3e,lad,red1} = & -\frac{i}{2\pi} \int \frac{d\omega}{(-\omega + i\varepsilon)^2} \sum_{a,b,b_1,v_1,i}^{i \neq b} \left[\frac{I_{vbb_1v_1}(\omega) I_{aiab}(0) I_{v_1b_1vi}(\omega) + I_{viv_1b_1}(\omega) I_{abai}(0) I_{v_1b_1vb}(\omega)}{\Delta_{bi}} \right. \\ & \left. + \frac{I_{vbb_1v_1}(\omega) I_{b_1aia}(0) I_{v_1ivb}(\omega) + I_{vbb_1i}(\omega) I_{iab_1a}(0) I_{v_1b_1vb}(\omega)}{(\Delta_{bi} + \omega + i\varepsilon)} \right], \end{aligned} \quad (C10)$$

$$\begin{aligned} \Delta E_{v, S(VP)EVP, IR \text{ div}}^{(3I)3e,lad,red1} = & -\frac{i}{2\pi} \int \frac{d\omega}{(-\omega + i\varepsilon)^2} \sum_{a,b,b_1,v_1,i}^{i \neq v} \left[\frac{I_{vaia}(0) I_{ibv_1b_1}(\omega) I_{b_1v_1bv}(\omega) + I_{vbb_1v_1}(\omega) I_{v_1b_1ib}(\omega) I_{aiav}(0)}{\Delta_{vi}} \right. \\ & \left. + \frac{I_{vbib_1}(\omega) I_{iav_1a}(0) I_{b_1v_1bv}(\omega) + I_{vbb_1b_1}(\omega) I_{v_1aia}(0) I_{b_1ibv}(\omega)}{(\Delta_{vi} - \omega + i\varepsilon)} \right], \end{aligned} \quad (C11)$$

for the IR divergent part. The IR finite part is further separated, because its first part is the counterpart of the previously introduced IR divergent terms,

$$\begin{aligned} \Delta E_{v, S[V(VP)P]E, IR \text{ free}}^{(3I)3e,lad,red1} = & -\frac{i}{4\pi} \int d\omega \left[\frac{1}{(\Delta_{vb} - \omega + i\varepsilon)^2} + \frac{1}{(\Delta_{vb} - \omega - i\varepsilon)^2} \right] \\ & \times \left[\sum_{a,b,b_1,v_1,i}^{i \neq v} \frac{I_{vbb_1v_1}(\omega) I_{v_1aia}(0) I_{b_1ivb}(\omega) + I_{vbb_1i}(\omega) I_{iav_1a}(0) I_{b_1v_1vb}(\omega)}{(\Delta_{bi} + \omega + i\varepsilon)} \right. \\ & \left. + \sum_{a,b,b_1,v_1,i}^{i \neq b} \frac{I_{vbb_1v_1}(\omega) I_{aiab}(0) I_{b_1v_1vi}(\omega) + I_{vib_1v_1}(\omega) I_{abai}(0) I_{b_1v_1vb}(\omega)}{\Delta_{bi}} \right], \end{aligned} \quad (C12)$$

$$\begin{aligned} \Delta E_{v, S[\text{VP}]\text{EVP}, \text{IR free}}^{(31)3e, \text{lad}, \text{red1}} &= -\frac{i}{4\pi} \int d\omega \left[\frac{1}{(\Delta_{vb} - \omega + i\varepsilon)^2} + \frac{1}{(\Delta_{vb} - \omega - i\varepsilon)^2} \right] \\ &\times \left[\sum_{a, b, b_1, v_1, i}^{i \neq v} \frac{I_{vaia}(0) I_{ibb_1 v_1}(\omega) I_{v_1 b_1 b v}(\omega) + I_{vbb_1 v_1}(\omega) I_{b_1 v_1 i b}(\omega) I_{aia v}(0)}{\Delta_{vi}} \right. \\ &\left. + \sum_{a, b, b_1, v_1, i}^{i \neq b} \frac{I_{vbb_1 v}(\omega) I_{b_1 aia}(0) I_{v_1 i b v}(\omega) + I_{vbi v_1}(\omega) I_{iab_1 a}(0) I_{v_1 b_1 b v}(\omega)}{(\Delta_{vi} - \omega + i\varepsilon)} \right], \end{aligned} \quad (\text{C13})$$

while its second part is simply the terms excluded in sums of certain diagrams,

$$\Delta E_{v, S[\text{V}(\text{VP})\text{P]E}, \text{IR free}}^{(31)3e, \text{lad}, \text{red1}} \omega = -\frac{i}{2\pi} \int d\omega \sum_{a, b, b_1, i, j}^{\{i, j\} \neq \{v, b\}} \frac{I_{vbi j}(\omega) I_{ab_1 ab}(0) I_{ij v b_1}(\omega)}{(\varepsilon_v - \omega - \varepsilon_i u)(\varepsilon_b + \omega - \varepsilon_j u)^2}, \quad (\text{C14})$$

$$\Delta E_{v, S[\text{VP}]\text{EVP}, \text{IR free}}^{(31)3e, \text{lad}, \text{red1}} \omega = -\frac{i}{2\pi} \int d\omega \sum_{a, b, v_1, i, j}^{\{i, j\} \neq \{v, b\}} \frac{I_{vbi j}(\omega) I_{ij v_1 b}(\omega) I_{av_1 av}(0)}{(\varepsilon_v - \omega - \varepsilon_i u)^2 (\varepsilon_b + \omega - \varepsilon_j u)}. \quad (\text{C15})$$

3. Reducible 2 terms

Facing now the reducible 2 contribution, the identical separation into IR divergent and IR free terms is conducted, on the top of the distinction among the two different subsets. The IR divergent terms are

$$\Delta E_{v, S[\text{V}(\text{VP})\text{P]E}, \text{IR div}}^{(31)3e, \text{lad}, \text{red2}} = \frac{i}{2\pi} \int \frac{d\omega}{(-\omega + i\varepsilon)^3} \sum_{a, b, b_1, b_2, v_1} [I_{vbb_1 v_1}(\omega) I_{b_1 ab_2 a}(0) I_{v_1 b_2 v b}(\omega) - I_{vbb_1 v_1}(\omega) I_{ab_1 ab}(0) I_{v_1 b_2 v b_1}(\omega)], \quad (\text{C16})$$

$$\Delta E_{v, S[\text{VP}]\text{EVP}, \text{IR div}}^{(31)3e, \text{lad}, \text{red2}} = \frac{i}{2\pi} \int \frac{d\omega}{(-\omega + i\varepsilon)^3} \sum_{a, b, b_1, v_1, v_2} [I_{vbb_1 v_1}(\omega) I_{v_1 b_1 v_2 b}(\omega) I_{av_2 av}(0) - I_{vbb_1 v_1}(\omega) I_{v_1 av_2 a}(0) I_{b_1 v_2 b v}(\omega)], \quad (\text{C17})$$

and the IR free ones are

$$\begin{aligned} \Delta E_{v, S[\text{V}(\text{VP})\text{P]E}, \text{IR free}}^{(31)3e, \text{lad}, \text{red2}} &= \frac{i}{4\pi} \int d\omega \left[\frac{1}{(\Delta_{vb} - \omega + i\varepsilon)^3} + \frac{1}{(\Delta_{vb} - \omega - i\varepsilon)^3} \right] \left[\sum_{a, b, b_1, v_1, v_2} I_{vbb_1 v_1}(\omega) I_{v_1 av_2 a}(0) I_{b_1 v_2 v b}(\omega) \right. \\ &\left. - \sum_{a, b, b_1, b_2, v_1} I_{vbb_2 v_1}(\omega) I_{ab_1 ab}(0) I_{b_2 v_1 v b_1}(\omega) \right], \end{aligned} \quad (\text{C18})$$

$$\begin{aligned} \Delta E_{v, S[\text{VP}]\text{EVP}, \text{IR free}}^{(31)3e, \text{lad}, \text{red2}} &= \frac{i}{4\pi} \int d\omega \left[\frac{1}{(\Delta_{vb} - \omega + i\varepsilon)^3} + \frac{1}{(\Delta_{vb} - \omega - i\varepsilon)^3} \right] \left[\sum_{a, b, b_1, v_1, v_2} I_{vbb_1 v_1}(\omega) I_{b_1 v_1 v_2 b}(\omega) I_{av_2 av}(0) \right. \\ &\left. - \sum_{a, b, b_1, b_2, v_1} I_{vbb_1 v_1}(\omega) I_{b_2 v_1 v b}(\omega) I_{b_1 ab_2 a}(0) \right]. \end{aligned} \quad (\text{C19})$$

4. Extra terms

The remaining terms

$$\Delta E_{v, S[\text{V}(\text{VP})\text{P]E}}^{(31)3e, \text{red1}} = \sum_{a, b, b_1, v_1, i}^{i \neq v} \frac{I_{vbb_1 v_1}(\Delta_{vb}) I_{v_1 aia}(0) I_{ib_1 v}(\Delta_{vb})}{(\varepsilon_v - \varepsilon_i)^2}, \quad (\text{C20})$$

and

$$\Delta E_{v, S[\text{VP}]\text{EVP}}^{(31)3e, \text{red1}} = -\sum_{a, b, b_1, v_1, i}^{i \neq b} \frac{I_{vbb_1 v_1}(\Delta_{vb}) I_{b_1 aia}(0) I_{iv_1 v}(\Delta_{vb})}{(\varepsilon_b - \varepsilon_i)^2}, \quad (\text{C21})$$

are not found via the perturbative analysis but are present in the redefined vacuum state approach. They are obtained as the interplay among terms generated from the ladder reducible 1 terms, upon the symmetrization of the energy flow in the loop, and four-electron reducible 1 terms. The former originates from H_1 while the latter originates from F_2 . They look like four-electron reducible 1 contribution, due to the absence of the ω integration. According to the gauge invariance of the three-electron S(VP)E subset of the two-photon-exchange corrections, they should be incorporated in the three-electron contribution of the three-photon-exchange corrections. The structure of these terms suggests then to be included in the reducible 1 contribution.

Appendix D: Third-order interelectronic corrections derived by a perturbative treatment: four-electron subset

One perturbs the S(VP)E three-electron expressions (14, 15) according to Eqs. (33–36) and finds, under the replacement (37), three different types of four-electron contribution: irreducible (irr), reducible 1 (red1) and reducible 2 (red2). They are displayed below, and furthermore separated into S(V(VP)P)E and S(VP)VP subsets. This separation relies on the redefined vacuum state analysis and its comparison with the perturbative one.

1. Irreducible terms

The four-electron irreducible contribution is found to be

$$\begin{aligned}
\Delta E_{v, \text{S(VP)EVP}}^{(31)4e, \text{irr}} = & - \sum_{a,b,c,i,j}^{j \neq v, (i,c) \neq (v,b)} \left\{ \frac{I_{ava_j}(0) [I_{jbci}(\Delta_{vc})I_{civb}(\Delta_{vc}) + I_{jbic}(\Delta_{cb})I_{icvb}(\Delta_{cb})]}{(\epsilon_v + \epsilon_b - \epsilon_c - \epsilon_i)(\epsilon_v - \epsilon_j)} \right. \\
& + \left. \frac{[I_{cijb}(\Delta_{vc})I_{vbci}(\Delta_{vc}) + I_{vbic}(\Delta_{cb})I_{icjb}(\Delta_{cb})] I_{java}(0)}{(\epsilon_v + \epsilon_b - \epsilon_c - \epsilon_i)(\epsilon_v - \epsilon_j)} \right\} \\
& - \sum_{a,b,c,i,j}^{j \neq v} \frac{I_{ava_j}(0)I_{jicb}(\Delta_{vc})I_{cbvi}(\Delta_{vc}) + I_{vicb}(\Delta_{vc})I_{cbji}(\Delta_{vc})I_{java}(0)}{(\epsilon_b + \epsilon_c - \epsilon_v - \epsilon_i)(\epsilon_v - \epsilon_j)} \\
& - \sum_{a,b,c,i,j}^{j \neq c} \frac{I_{vijb}(\Delta_{vc})I_{jaca}(0)I_{cbvi}(\Delta_{vc}) + I_{vicb}(\Delta_{vc})I_{acaj}(0)I_{jbvi}(\Delta_{vc})}{(\epsilon_b + \epsilon_c - \epsilon_v - \epsilon_i)(\epsilon_c - \epsilon_j)} \\
& - \sum_{a,b,c,i,j}^{j \neq c, (i,c) \neq (v,b)} \frac{I_{acaj}(0)I_{vbci}(\Delta_{vc})I_{jivb}(\Delta_{vc}) + I_{vbji}(\Delta_{vc})I_{civb}(\Delta_{vc})I_{jaca}(0)}{(\epsilon_v + \epsilon_b - \epsilon_c - \epsilon_i)(\epsilon_c - \epsilon_j)} \\
& - \sum_{i,j} \frac{I_{vicb}(\Delta_{vc})I_{iaja}(0)I_{cbvj}(\Delta_{vc})}{(\epsilon_b + \epsilon_c - \epsilon_v - \epsilon_i)(\epsilon_b + \epsilon_c - \epsilon_v - \epsilon_j)}, \tag{D1}
\end{aligned}$$

for the S(VP)EVP subset and,

$$\begin{aligned}
\Delta E_{v, \text{S[V(VP)P]E}}^{(31)4e, \text{irr}} = & - \sum_{a,b,c,i,j}^{j \neq b, (i,c) \neq (v,b)} \left\{ \frac{I_{aba_j}(0) [I_{vjci}(\Delta_{vc})I_{civb}(\Delta_{vc}) + I_{vjic}(\Delta_{cb})I_{icvb}(\Delta_{cb})]}{(\epsilon_v + \epsilon_b - \epsilon_c - \epsilon_i)(\epsilon_b - \epsilon_j)} \right. \\
& + \left. \frac{[I_{civj}(\Delta_{vc})I_{vbci}(\Delta_{vc}) + I_{vbic}(\Delta_{cb})I_{icvj}(\Delta_{cb})] I_{jaba}(0)}{(\epsilon_v + \epsilon_b - \epsilon_c - \epsilon_i)(\epsilon_b - \epsilon_j)} \right\} \\
& - \sum_{a,b,c,i,j}^{j \neq b} \frac{I_{vicj}(\Delta_{vc})I_{jaba}(0)I_{cbvi}(\Delta_{vc}) + I_{vicb}(\Delta_{vc})I_{abaj}(0)I_{cjvi}(\Delta_{vc})}{(\epsilon_b + \epsilon_c - \epsilon_v - \epsilon_i)(\epsilon_b - \epsilon_j)} \\
& - \sum_{a,b,c,i,j}^{(i,c) \neq (v,b), (j,c) \neq (v,b)} \frac{I_{vbci}(\Delta_{vc})I_{iaja}(0)I_{cjvb}(\Delta_{vc}) + I_{vbic}(\Delta_{cb})I_{iaja}(0)I_{jcvb}(\Delta_{cb})}{(\epsilon_v + \epsilon_b - \epsilon_c - \epsilon_i)(\epsilon_v + \epsilon_b - \epsilon_c - \epsilon_j)} \\
& - \sum_{a,b,c,i,j}^{j \neq c, (i,c) \neq (v,b)} \frac{I_{vbij}(\Delta_{cb})I_{icvb}(\Delta_{cb})I_{jaca}(0) + I_{acaj}(0)I_{vbic}(\Delta_{cb})I_{jivb}(\Delta_{cb})}{(\epsilon_v + \epsilon_b - \epsilon_c - \epsilon_i)(\epsilon_c - \epsilon_j)}, \tag{D2}
\end{aligned}$$

for the S[V(VP)P]E one.

2. Reducible 1 terms

The reducible 1 contribution is also split into S(VP)EVP and S[V(VP)P]E subsets, respectively, and can be cast in the form

$$\begin{aligned}
\Delta E_{v, \text{S(VP)EVP}}^{(3\text{I})4\text{e,red1}} = & - \sum_{a,b,b_1,v_1,i}^{i \neq b} \frac{I_{vbb_1v_1}(\Delta_{vb})I_{ab_1ai}(0)I'_{iv_1vb}(\Delta_{vb}) + I_{abai}(0)I_{vib_1v_1}(\Delta_{vb})I'_{b_1v_1vb}(\Delta_{vb})}{(\epsilon_b - \epsilon_i)} \\
& - \sum_{a,b,b_1,v_1,i}^{i \neq v} \frac{I_{vbb_1i}(\Delta_{vb})I_{iav_1a}(0)I'_{b_1v_1vb}(\Delta_{vb}) + I_{vbb_1v_1}(\Delta_{vb})I'_{b_1v_1ib}(\Delta_{vb})I_{iava}(0)}{(\epsilon_v - \epsilon_i)} \\
& - \sum_{a,b,c,v_1,i}^{(i,c) \neq (v,b)} \frac{[I_{vbc_i}(\Delta_{vc})I'_{civb}(\Delta_{vc}) + I'_{vbc_i}(\Delta_{vc})I_{civb}(\Delta_{vc})] I_{v_1av_1a}(0)}{(\epsilon_v + \epsilon_b - \epsilon_c - \epsilon_i)} \\
& + \sum_{a,b,c,c_1,i}^{(i,c) \neq (v,b)} \frac{[I_{vbc_i}(\Delta_{vc})I'_{civb}(\Delta_{vc}) + I'_{vbc_i}(\Delta_{vc})I_{civb}(\Delta_{vc})] I_{c_1ac_1a}(0)}{(\epsilon_v + \epsilon_b - \epsilon_c - \epsilon_i)} \\
& - \sum_{a,b,c,v_1,i} \frac{[I_{vicb}(\Delta_{vc})I'_{cbvi}(\Delta_{vc}) + I'_{vicb}(\Delta_{vc})I_{cbvi}(\Delta_{vc})] I_{v_1av_1a}(0)}{(\epsilon_b + \epsilon_c - \epsilon_v - \epsilon_i)} \\
& + \sum_{a,b,c,c_1,i} \frac{[I_{vicb}(\Delta_{vc})I'_{cbvi}(\Delta_{vc}) + I'_{vicb}(\Delta_{vc})I_{cbvi}(\Delta_{vc})] I_{c_1ac_1a}(0)}{(\epsilon_b + \epsilon_c - \epsilon_v - \epsilon_i)} \\
& + \sum_{a,b,c,v_1,i}^{(i,c) \neq (v,b)} \frac{I_{v_1av_1a}(0) [I_{vbc_i}(\Delta_{vc})I_{civb}(\Delta_{vc}) + I_{vbc_i}(\Delta_{cb})I_{civb}(\Delta_{cb})]}{(\epsilon_v + \epsilon_b - \epsilon_c - \epsilon_i)^2} \\
& - \sum_{a,b,c,v_1,i} \frac{I_{v_1av_1a}(0)I_{vicb}(\Delta_{vc})I_{cbvi}(\Delta_{vc})}{(\epsilon_b + \epsilon_c - \epsilon_v - \epsilon_i)^2} \\
& + \sum_{a,b,c,c_1,i} \frac{I_{c_1ac_1a}(0)I_{vicb}(\Delta_{vc})I_{cbvi}(\Delta_{vc})}{(\epsilon_b + \epsilon_c - \epsilon_v - \epsilon_i)^2} \\
& - \sum_{a,b,c,c_1,i}^{(i,c) \neq (v,b)} \frac{I_{c_1ac_1a}(0)I_{vbc_i}(\Delta_{vc})I_{civb}(\Delta_{vc})}{(\epsilon_v + \epsilon_b - \epsilon_c - \epsilon_i)^2}, \tag{D3}
\end{aligned}$$

and

$$\begin{aligned}
\Delta E_{v, \text{S[V(VP)P]E}}^{(3\text{I})4\text{e,red1}} = & - \sum_{a,b,b_1,v_1,i}^{i \neq v} \frac{I_{avai}(0)I_{ibb_1v_1}(\Delta_{vb})I'_{b_1v_1vb}(\Delta_{vb}) + I_{vbb_1v_1}(\Delta_{vb})I_{av_1ai}(0)I'_{b_1ivb}(\Delta_{vb})}{(\epsilon_v - \epsilon_i)} \\
& - \sum_{a,b,b_1,v_1,i}^{i \neq b} \frac{I_{vbb_1v_1}(\Delta_{vb})I'_{b_1v_1vi}(\Delta_{vb})I_{iaba}(0) + I_{vbiv_1}(\Delta_{vb})I_{iab_1a}(0)I'_{b_1v_1vb}(\Delta_{vb})}{(\epsilon_b - \epsilon_i)} \\
& - \sum_{a,b,c,c_1,i}^{(i,c) \neq (v,b)} \frac{[I_{vbic}(\Delta_{cb})I'_{icvb}(\Delta_{cb}) + I'_{vbic}(\Delta_{cb})I_{icvb}(\Delta_{cb})] I_{c_1ac_1}(0)}{(\epsilon_v + \epsilon_b - \epsilon_c - \epsilon_i)} \\
& + \sum_{a,b,c,b_1,i}^{(i,c) \neq (v,b)} \frac{[I_{vbic}(\Delta_{cb})I'_{icvb}(\Delta_{cb}) + I'_{vbic}(\Delta_{cb})I_{icvb}(\Delta_{cb})] I_{b_1ab_1a}(0)}{(\epsilon_v + \epsilon_b - \epsilon_c - \epsilon_i)} \\
& + \sum_{a,b,c,b_1,i}^{(i,c) \neq (v,b)} \frac{I_{b_1ab_1a}(0) [I_{vbc_i}(\Delta_{vc})I_{civb}(\Delta_{vc}) + I_{vbc_i}(\Delta_{cb})I_{civb}(\Delta_{cb})]}{(\epsilon_v + \epsilon_b - \epsilon_c - \epsilon_i)^2} \\
& + \sum_{a,b,c,b_1,i} \frac{I_{b_1ab_1a}(0)I_{vicb}(\Delta_{vc})I_{cbvi}(\Delta_{vc})}{(\epsilon_b + \epsilon_c - \epsilon_v - \epsilon_i)^2} \\
& - \sum_{a,b,c,c_1,i}^{(i,c) \neq (v,b)} \frac{I_{c_1ac_1a}(0)I_{vbic}(\Delta_{cb})I_{icvb}(\Delta_{cb})}{(\epsilon_v + \epsilon_b - \epsilon_c - \epsilon_i)^2}. \tag{D4}
\end{aligned}$$

3. Reducible 2 terms

Each of the inspected subset participates equally to the reducible 2 contribution. One finds

$$\begin{aligned} \Delta E_{v, S(\text{VP})\text{EVP}}^{(3\text{I})4\text{e,red2}} &= -\frac{1}{2} \sum_{a,b,b_1,v_1,v_2} [I_{vbb_1v_1}(\Delta_{vb})I''_{b_1v_1vb}(\Delta_{vb}) + I'_{vbb_1v_1}(\Delta_{vb})I'_{b_1v_1vb}] I_{v_2av_2a}(0) \\ &+ \frac{1}{2} \sum_{a,b,b_1,b_2,v_1} [I_{vbb_1v_1}(\Delta_{vb})I''_{b_1v_1vb}(\Delta_{vb}) + I'_{vbb_1v_1}(\Delta_{vb})I'_{b_1v_1vb}] I_{b_2ab_2a}(0), \end{aligned} \quad (\text{D5})$$

originated from the H diagrams, as well as

$$\begin{aligned} \Delta E_{v, S[\text{V}(\text{VP})\text{P}]E}^{(3\text{I})4\text{e,red2}} &= -\frac{1}{2} \sum_{a,b,b_1,v_1,v_2} [I_{vbb_1v_1}(\Delta_{vb})I''_{b_1v_1vb}(\Delta_{vb}) + I'_{vbb_1v_1}(\Delta_{vb})I'_{b_1v_1vb}] I_{v_2av_2a}(0) \\ &+ \frac{1}{2} \sum_{a,b,b_1,b_2,v_1} [I_{vbb_1v_1}(\Delta_{vb})I''_{b_1v_1vb}(\Delta_{vb}) + I'_{vbb_1v_1}(\Delta_{vb})I'_{b_1v_1vb}] I_{b_2ab_2a}(0), \end{aligned} \quad (\text{D6})$$

for the F diagrams.

Appendix E: Symmetry argument for vanishing ladder reducible 2 terms

The cancellation of the $1/\mu$ IR divergence in ladder reducible 2 terms was shown in Table I. This was achieved by searching for a compensating term within the subset of the investigated term. A symmetry argument might also rule out this issue at the individual Feynman diagram level, without the need of a term to absorb its divergence. The naive way to argue would be as follows. Recall that in Feynman gauge, $I(\omega)$ is a symmetric operator. Therefore, when the IR divergence is met in the ladder reducible 2 term, one faces a symmetric numerator divided by an anti-symmetric denominator integrated over a symmetric interval. It vanishes due to parity consideration. However, the problem is that the $i\varepsilon$ prescription spoils the anti-symmetric behaviour of the denominator. Hence, a Wick rotation is applied and the expression looks as

$$\begin{aligned} \frac{i}{2\pi} \int_{-\infty}^{\infty} d\omega \frac{I(\omega)I(\omega)I(0)}{(-\omega + i\varepsilon)^3} &= \\ \frac{-I(0)}{2\pi} \mathcal{P} \int_0^{i\infty} d\omega_E \frac{I(-i\omega_E)I(-i\omega_E) - I(i\omega_E)I(i\omega_E)}{(i\omega_E)^3} &\propto \\ \frac{-i}{2\pi} I(0) \mathcal{P} \int_0^{i\infty} d\omega_E \frac{2 \sinh \omega_E R}{\omega_E^3} &\stackrel{\text{B.H}}{=} \\ \frac{-iR}{3\pi} I(0) \mathcal{P} \int_0^{i\infty} d\omega_E \frac{\cosh \omega_E R}{\omega_E^2} &\stackrel{\text{Taylor}}{\approx} \\ \frac{-iR}{3\pi} I(0) \mathcal{P} \int_0^{i\infty} d\omega_E \left[\frac{1}{\omega_E^2} + \frac{1}{2!} R^2 \right] & \quad (\text{E1}) \end{aligned}$$

Only the principal value is considered since the third order pole does not contribute to the pole term. One can take the exponential terms of the interelectronic operators out and rephrase them as a hyperbolic sine. Then, Bernoulli-L'Hospital rule is applied once and the hyperbolic cosine is Taylor expanded, as the interest lies in the low-energy limit. Here R stands for $R = r_{12} + r_{34}$. An interesting feature is seen at this point, it leads to a pure imaginary end result. Furthermore, one retrieves the $1/\mu$ divergent behavior encountered previously. The imaginary contribution to the energy, the decay rate, accounts for the possible instability of the excited states. Since the interest lies in the energy level and not its lifetime, one can neglect it. For completeness, if the ground state is under consideration, it features obviously no instabilities.

[1] X. Fan, T. G. Myers, B. A. D. Sukra, and G. Gabrielse, Phys. Rev. Lett. **130**, 071801 (2023).

[2] The authors of Ref. [1] stated that the first four expansion's coefficients C_i , $i = 2, 4, 6, 8$ are known exactly but the last one, C_{10} , was required and had to be calculated numerically in order

- to catch up with the precision of the measurements.
- [3] T. Sailer, V. Debieerre, Z. Harman, F. Heiße, C. König, J. Morgner, B. Tu, A. V. Volotka, C. H. Keitel, K. Blaum, et al., *Nature* **606**, 479 (2022).
- [4] M. G. Kozlov, M. S. Safronova, J. R. Crespo López-Urrutia, and P. O. Schmidt, *Rev. Mod. Phys.* **90**, 045005 (2018).
- [5] P. Indelicato, *J. Phys. B* **52**, 232001 (2019).
- [6] A. Gumberidze, T. Stöhlker, D. Banaś, K. Beckert, P. Beller, H. F. Beyer, F. Bosch, S. Hagmann, C. Kozhuharov, D. Liesen, et al., *Phys. Rev. Lett.* **94**, 223001 (2005).
- [7] V. A. Yerokhin, P. Indelicato, and V. M. Shabaev, *Phys. Rev. Lett.* **91**, 073001 (2003).
- [8] T. Gassner, M. Trassinelli, R. Heß, U. Spillmann, D. Banaś, K.-H. Blumenhagen, F. Bosch, C. Brandau, W. Chen, C. Dimopoulou, et al., *New J. Phys.* **20**, 073033 (2018).
- [9] P. Amaro, S. Schlessler, M. Guerra, E.-O. Le Bigot, J.-M. Isac, P. Travers, J. P. Santos, C. I. Szabo, A. Gumberidze, and P. Indelicato, *Phys. Rev. Lett.* **109**, 043005 (2012).
- [10] S. W. Epp, R. Steinbrügge, S. Bernitt, J. K. Rudolph, C. Beilmann, H. Bekker, A. Müller, O. O. Versolato, H.-C. Wille, H. Yavaş, et al., *Phys. Rev. A* **92**, 020502 (2015).
- [11] C. Brandau, C. Kozhuharov, A. Müller, W. Shi, S. Shippers, T. Bartsch, S. Böhm, C. Böhme, A. Hoffknecht, H. Knopp, et al., *Phys. Rev. Lett.* **91**, 073202 (2003).
- [12] P. Beiersdorfer, H. Chen, D. B. Thorn, and E. Träbert, *Phys. Rev. Lett.* **95**, 233003 (2005).
- [13] D. Bernhardt, C. Brandau, Z. Harman, C. Kozhuharov, S. Böhm, F. Bosch, S. Fritzsche, J. Jacobi, S. Kieslich, H. Knopp, et al., *Phys. Rev. A* **91**, 012710 (2015).
- [14] D. Bernhardt, C. Brandau, Z. Harman, C. Kozhuharov, S. Böhm, F. Bosch, S. Fritzsche, J. Jacobi, S. Kieslich, H. Knopp, et al., *J. Phys. B: At., Mol. Opt. Phys.* **48**, 144008 (2015).
- [15] I. Draganić, J. R. Crespo López-Urrutia, R. DuBois, S. Fritzsche, V. M. Shabaev, R. Soria Orts, I. I. Tupitsyn, Y. Zou, and J. Ullrich, *Phys. Rev. Lett.* **91**, 183001 (2003).
- [16] V. Mäckel, R. Klawitter, G. Brenner, J. R. Crespo López-Urrutia, and J. Ullrich, *Phys. Rev. Lett.* **107**, 143002 (2011).
- [17] Q. Lu, C. L. Yan, G. Q. Xu, N. Fu, Y. Yang, Y. Zou, A. V. Volotka, J. Xiao, N. Nakamura, and R. Hutton, *Phys. Rev. A* **102**, 042817 (2020).
- [18] G. O’Neil, S. Sanders, P. Szypryt, Dipti, A. Gall, Y. Yang, S. M. Brewer, R. Doriese, J. Fowler, A. Naing, et al., *Phys. Rev. A* **102**, 032803 (2020).
- [19] M. H. Chen, K. T. Cheng, P. Beiersdorfer, and J. Sapirstein, *Phys. Rev. A* **68**, 022507 (2003).
- [20] P. Beiersdorfer, A. L. Osterheld, J. H. Scofield, J. R. Crespo López-Urrutia, and K. Widmann, *Phys. Rev. Lett.* **80**, 3022 (1998).
- [21] S. A. Blundell, P. J. Mohr, W. R. Johnson, and J. Sapirstein, *Phys. Rev. A* **48**, 2615 (1993).
- [22] J. Sapirstein and K. T. Cheng, *Phys. Rev. A* **91**, 062508 (2015).
- [23] V. M. Shabaev and I. G. Fokeeva, *Phys. Rev. A* **49**, 4489 (1994).
- [24] V. M. Shabaev, *Phys. Rep.* **356**, 119 (2002).
- [25] R. N. Soguel, A. V. Volotka, E. V. Tryapitsyna, D. A. Glazov, V. P. Kosheleva, and S. Fritzsche, *Phys. Rev. A* **103**, 042818 (2021).
- [26] R. N. Soguel, A. V. Volotka, and S. Fritzsche, *Phys. Rev. A* **106**, 012802 (2022).
- [27] A. V. Volotka, D. A. Glazov, V. M. Shabaev, I. I. Tupitsyn, and G. Plunien, *Phys. Rev. Lett.* **103**, 033005 (2009).
- [28] D. A. Glazov, A. V. Volotka, V. M. Shabaev, I. I. Tupitsyn, and G. Plunien, *Phys. Rev. A* **81**, 062112 (2010).
- [29] A. V. Volotka, D. A. Glazov, O. V. Andreev, V. M. Shabaev, I. I. Tupitsyn, and G. Plunien, *Phys. Rev. Lett.* **108**, 073001 (2012).
- [30] A. V. Volotka, D. A. Glazov, V. M. Shabaev, I. I. Tupitsyn, and G. Plunien, *Phys. Rev. Lett.* **112**, 253004 (2014).
- [31] D. A. Glazov, F. Köhler-Langes, A. V. Volotka, K. Blaum, F. Heiße, G. Plunien, W. Quint, S. Rau, V. M. Shabaev, S. Sturm, et al., *Phys. Rev. Lett.* **123**, 173001 (2019).
- [32] V. P. Kosheleva, A. V. Volotka, D. A. Glazov, and S. Fritzsche, *Phys. Rev. Research* **2**, 013364 (2020).
- [33] A. V. Malyshev, A. V. Volotka, D. A. Glazov, I. I. Tupitsyn, V. M. Shabaev, and G. Plunien, *Phys. Rev. A* **90**, 062517 (2014).
- [34] A. V. Malyshev, A. V. Volotka, D. A. Glazov, I. I. Tupitsyn, V. M. Shabaev, and G. Plunien, *Phys. Rev. A* **92**, 012514 (2015).
- [35] A. V. Malyshev, D. A. Glazov, Y. S. Kozhedub, I. S. Anisimova, M. Y. Kaygorodov, V. M. Shabaev, and I. I. Tupitsyn, *Phys. Rev. Lett.* **126**, 183001 (2021).
- [36] J. Sommerfeldt, V. A. Yerokhin, T. Stöhlker, and A. Surzhykov, *Phys. Rev. Lett.* **131**, 061601 (2023).
- [37] S. Weinberg, *The Quantum Theory of Fields*, vol. 1 (Cambridge University Press, 1995).
- [38] W. H. Furry, *Phys. Rev.* **81**, 115 (1951).
- [39] I. Lindgren and J. Morrison, *Atomic Many-Body Theory* (Springer-Verlag, Berlin, 1985).
- [40] W. R. Johnson, *Atomic Structure Theory. Lectures on Atomic Physics* (Springer-Verlag, Berlin, Heidelberg, 2007).
- [41] R. N. Soguel, A. V. Volotka, D. A. Glazov, and S. Fritzsche, *Symmetry* **13** (2021), ISSN 2073-8994.
- [42] P. J. Mohr, G. Plunien, and G. Soff, *Phys. Rep.* **293**, 227 (1998).
- [43] I. Lindgren, S. Salomonson, and B. Åsén, *Phys. Rep.* **389**, 161 (2004).
- [44] O. Yu. Andreev, L. N. Labzowsky, G. Plunien, and D. A. Solov'yev, *Phys. Rep.* **455**, 135 (2008).
- [45] V. A. Yerokhin, P. Indelicato, and V. M. Shabaev, *Phys. Rev. Lett.* **97**, 253004 (2006).
- [46] See below Eq. (54) and Eq. (63), respectively, in [25].
- [47] V. A. Yerokhin, C. H. Keitel, and Z. Harman, *Phys. Rev. A* **104**, 022814 (2021).
- [48] V. A. Yerokhin, K. Pachucki, M. Puchalski, C. H. Keitel, and Z. Harman, *Phys. Rev. A* **102**, 022815 (2020).
- [49] E. H. Wichmann and N. M. Kroll, *Phys. Rev.* **101**, 843 (1956).
- [50] A potential which accounts for a partial two-loop (second order in α) VP correction is the Källén-Sabry potential [56–60].
- [51] E. A. Uehling, *Phys. Rev.* **48**, 55 (1935).
- [52] V. A. Yerokhin, A. N. Artemyev, V. M. Shabaev, M. M. Sysak, O. M. Zhrebtsov, and G. Soff, *Phys. Rev. A* **64**, 032109 (2001).
- [53] I. S. Gradshteyn, I. M. Ryzhik, A. Jeffrey, and D. Zwillinger, *Table of Integrals, Series, and Products* (2007).
- [54] J. Sapirstein and K. T. Cheng, *Phys. Rev. A* **83**, 012504 (2011).
- [55] A. Volotka, private communication.
- [56] G. Kallen and A. Sabry, *Selsk. Mat.—Fys. Medd* **29**, 17 (1955).
- [57] R. Barbieri, J. Mignaco, and E. Remiddi, *Lettere al Nuovo Cimento* (1969-1970) **3**, 588 (1970).
- [58] R. Barbieri, J. Mignaco, and E. Remiddi, *Nuovo Cimento. A* **11**, 824 (1972).
- [59] R. Barbieri, J. Mignaco, and E. Remiddi, *Nuovo Cimento A Serie* **11**, 865 (1972).
- [60] R. Barbieri and E. Remiddi, *Nuovo Cimento. A* **13**, 99 (1973).
- [61] See remarks below Eqs. (32, 35, 37) in Ref. [47].
- [62] The same problem was met when comparing the two-photon-exchange expressions with the ones derived by Sapirstein and Cheng, see below Eq. (79) in [25].
- [63] See [61].
- [64] See [62].